6-1974

The Ductile-Brittle Fracture Transition: A Comparison of Macro and Microscopic Observation on Compact Tension Specimens

Wu-Sen Lin
University of Tennessee - Knoxville

To the Graduate Council:

I am submitting herewith a thesis written by Wu-Sen Lin entitled "The Ductile-Brittle Fracture Transition: A Comparison of Macro and Microscopic Observation on Compact Tension Specimens." I have examined the final electronic copy of this thesis for form and content and recommend that it be accepted in partial fulfillment of the requirements for the degree of Master of Science, with a major in Engineering Science.

William T. Becker, Major Professor

We have read this thesis and recommend its acceptance:

E. E. Stansbury, Archie Mathews

Accepted for the Council:
Dixie L. Thompson

Vice Provost and Dean of the Graduate School

(Original signatures are on file with official student records.)

March 13, 1974

To the Graduate Council:

I am submitting herewith a thesis written by Wun-Sen Lin entitled "The Ductile-Brittle Fracture Transition: A Comparison of Macro and Microscopic Observation on Compact Tension Specimens." I recommend that it be accepted for 15 quarter hours of credit in partial fulfillment of the requirements for the degree of Master of Science, with a major in Metallurgical Engineering.

William T. Becker
Major Professor

We have read this thesis and recommend its acceptance:

E. E. Stansbury

Archie Mathews

Accepted for the Council:

Hilton A. Smith
Vice Chancellor for Graduate Studies and Research

E

THE DUCTILE-BRITTLE FRACTURE TRANSITION: A COMPARISON OF MACRO AND MICROSCOPIC OBSERVATIONS ON COMPACT TENSION SPECIMENS

A Thesis

Presented to

the Graduate Council of

The University of Tennessee

In Partial Fulfillment

of the Requirements for the Degree

Master of Science

---

by

Wun-Sen Lin

June 1974

ACKNOWLEDGEMENT

The author wishes to express his sincere appreciation to Dr. W. T. Becker, his advisor, for his continued interest and guidance throughout this investigation. Without his enthusiasm, the progress of this work would have been considerably slower.

The author is grateful to the Department of Chemical and Metallurgical Engineering for providing financial aid. The author would like to comment on the excellent atmosphere that exists in the Department of Chemical and Metallurgical Engineering in terms of student-faculty contact and graduate student interaction.

Thanks also go to Dr. A. Mathews of Engineering Science and Mecahnics for his assistance during the course of this work.

Acknowledgement is extended to Ms. Bette Leonard for her speed and accuracy in preparing the manuscript.

Finally, the author wishes to express his appreciation to his parents, Mr. and Mrs. Wei-Song Lin for their encouragement during his graduate career.

ABSTRACT

Rapid development of failure analysis has brought increased attention to the concept of fracture toughness in recent years. The existing criteria for valid plane strain fracture toughness testing based on a macroscopic view have been shown to be conservative in some cases, and for other cases to be of questionable validity.

Compact tension specimens of variable thickness were fabricated from annealed O1 tool steel between 0.125 inch and 1.00 inch. Load-COD data and gross plastic flow measurements are compared to scanning electron microscopy (SEM) fracture surface analysis in order to correlate macroscopic observations of the ductile-brittle transition on a macroscopic scale with microscopic modes of failure. Comparisons of macroscopic and microscopic data permit the validity of macroscopic criteria for plane strain fracture toughness to be examined. Criteria examined include criteria based on continuum mechanics, shape of the load-crack opening displacement curve, plan view plastic zone size (PZS) and percent slant fracture.

Data indicate, for example, that PZS criteria need not be met in order to obtain totally brittle fracture on a microscopic scale, so that this criterion is conservative. Alternatively plane strain fracture toughness does decrease as the percent flat fracture approaches 100 percent, but SEM data indicate that 100 percent macroscopic flat fracture does not correspond to 100 percent microscopic brittle fracture at the minimum thickness required to obtain 100 percent

macroscopic flat fracture. This implies that a larger thickness is required than is indicated by macroscopic appearance and that larger thicknesses must be utilized to obtain a valid plane strain fracture toughness.

TABLE OF CONTENTS

LIST OF FIGURES

FIGURE PAGE

FIGURE PAGE

FIGURE PAGE

FIGURE PAGE

FIGURE PAGE

NOMENCLATURE

A = crack length.

B = thickness of the specimen.

E = Young's modulus.

K = fracture toughness parameter (stress intensity factor).

K_Q = apparent fracture toughness.

K_c = the plane stress value of K.

K_{Ic} = the plane strain value of K.

n = strain hardening coefficient.

P_p = proportional load on load-COD curve.

P_Q = Secant intercept load on load-COD curve.

P_m = maximum load on load-COD curve.

T = surface tension of the crack surface.

W = width of the specimen.

ν = Poisson's ratio.

σ = nominal stress.

σ^* = critical value of σ.

σ_y, σ_ℓ = stress in the load direction.

σ_x, σ_w = stress in the width direction.

σ_t = stress in the thickness direction.

τ_{xy} = shear stress on the xy plane.

γ_p = plastic zone correction factor.

COD = crack opening displacement

PIZ = plastic initiation zone.

SEM = scanning electron microscopy.

CHAPTER I

INTRODUCTION

Current trends in alloy development are toward higher specific strength and specific moduli materials. The application of these materials for structural design, particularly in the aerospace and pressure vessel fields, has brought increasing emphasis on the fracture behavior of these materials. Since fracture is known to occur--even for static loading at moderate temperatures--at stress levels lower than that of even the yield strength of the material, it is clear that the ultimate strength or the yield strength of the material may not be the correct mechanical property to determine maximum allowable loads. The ability of a material to withstand failure in the presence of defects such as cracks and notches is becoming recognized as a more meaningful concept upon which maximum allowable load calculations should be based. Fracture resistance depends ultimately on the ability of a material to resist crack nucleation and/or growth. The term "fracture toughtness" is used to describe that capability. If correctly interpreted, fracture toughness mechanical properties may be used to define the largest crack or other defect that a material can tolerate without fracture when loaded to a level approaching that at which it would fail by excessive plastic deformation (1). Alternatively, fracture toughness may be interpreted as defining the minimum energy required for crack initiation and a given mode of propagation. Recognizing the importance

of fracture toughness, the technology of fracture toughness testing, and the definition of new material constants based on fracture toughness testing has grown rapidly in recent years. Several material constants have been proposed, but most attention has been devoted to the plane stress stress intensity factor (K_c) and the plane strain stress intensity factor (K_{Ic}). (This is not to imply that these two material constants are indeed the best constants to characterize fracture toughness behavior.) The two stress intensity factors K_c and K_{Ic} predict the maximum nominal load and crack length that can be tolerated without ductile tearing (K_c), or without brittle fracture (K_{Ic}).

From a macroscopic viewpoint, crack growth velocities are known to increase as the nominal external loads increase in intensity, as the loading rate is increased, as the temperature is decreased, and as the ability of the material to plastically deform decreases. For a given material, the ability of plastically deform decreases due to increased stress state triaxiality which may be generated by either externally applied loads or developed internally due to geometry. The term "constraint" is used to describe the inability of an inherently ductile material to plastically deform due to the internal state of stress. Additionally, it is recognized that some materials have metallurgical structures that render the material incapable of deforming plastically even in the absence of imposed constraint. Since ductile failure--failure accompanied by macroscopic plastic flow--must be the result of crack propagation through work hardened material, it is reasonable to assume that ductile failure requires a higher energy,

occurs at a slower rate, and requires a higher stress intensity than does brittle fracture. These assumptions, in conjunction with the ease by which gross macroscopic flow may be monitored (visible distortion, strain gaging), make it most desirable to obtain a material parameter than characterizes the resistance of a material to brittle cataclysmic fracture. Such a parameter then provides a worst case of lower bound design criterion.

Plane Strain Fracture Toughness

The well known pendulum impact tests developed as a result of brittle fracture in Liberty ships were the first attempt to characterize brittle behavior of materials. Unfortunately, although these tests provide a minimum service temperature for ductile fracture, test results do not provide a simple means to calculate maximum allowable loads, nor do they predict material behavior in terms of crack length. Additionally, the pendulum tests are conducted at sufficiently high strain rates that data may well not reflect material behavior for some important practical applications (e.g., pressure vessel design).

Early theoretical work, devoted to predicting stress concentrations and triaxiality developed adjacent to defects, developed by workers in theory of elasticity and more recently continuum mechanics led to the development of the notch tensile test. This test dramatically demonstrates the loss of tensile ductility due to geometrical constraint (described as "notch sensitivity"). However, although the test does provide data in the form of nominal stress, it does not provide data in terms of critical crack length. The crack

opening fracture tests (bending and compact tension) developed in the last few years, on the other hand, do include parameters of crack length and nominal applied stress. Such tests have an associated predetermined initial stress concentration factor and can be conducted with temperature or initial strain rate as an independent variable. Such tests presumably measure minimum crack initiation energy plus propagation energy if starter crack is introduced in front of a stress intensifying notch by fatigue loading. Data from such tests can be used to estimate lower bound maximum nominal loads for a given crack length or vice versa. It is the fracture toughness tests, then, that provide the design engineer with a material constant formulated in terms of nominal applied load and crack length, in a simple expression. Not discounting the importance of the transition from ductile to brittle behavior with temperature which is revealed by the pendulum impact or drop weight tests, it is the simple form of the stress intensity factors derived from fracture toughness testing, and the direct application of the stress intensity factor to calculate maximum allowable loads and/or crack lengths, that make the stress intensity factors so appealing to the design engineer.

Considerable controversy exists in the literature as to the precautions that must be followed in experimental work to assure that the true fracture toughness has been measured. More interest has centered on the plane strain fracture toughness than the plane stress fracture toughness because the plane strain value is a lower bound value, and because of the greater experimental difficulty in measuring the plane stress value. Even though the plane strain value is

presumably easier to determine, the continually changing specifications contained in ASTM E-399 to determine the validity of a given test point out that the issue is far from settled even for this case.

Purpose of the Investigation

The difficulty in determining whether a valid test has been performed resides in the cyclic arguments associated with determining whether "brittle fracture" has occurred in the specimen. Brittle fracture is normally considered in a macroscopic sense and is taken to simultaneously mean, in a compact tension specimen, the absence of gross plastic flow and fracture on a plane normal to the applied load and parallel to the crack starter notch. The absence of plastic flow is assured by the absence of transverse strain in the specimen and the absence of a plastic hinge visible on the surface (plan view) of the specimen. Fracture on a plane oblique to the applied load is presumed to be ductile.

Alternatively, brittle fracture is assumed to have occurred if "pop-in" occurs during the course of the test. Pop-in refers to the audible sound sometimes heard when the crack rapidly accelerates. Pop-in also amounts to a temporary loss of strain control and load monitoring, and is recorded as a constant or decreasing value of load with crack opening displacement (COD) (Figure 1). This is in contrast to a steadily rising load with COD displacement which occurs with a slow ductile tearing mode of crack propagation. In practice, pop-in often causes only a temporary instability and the specimen does not completely fracture. It is also possible that the amount of brittle

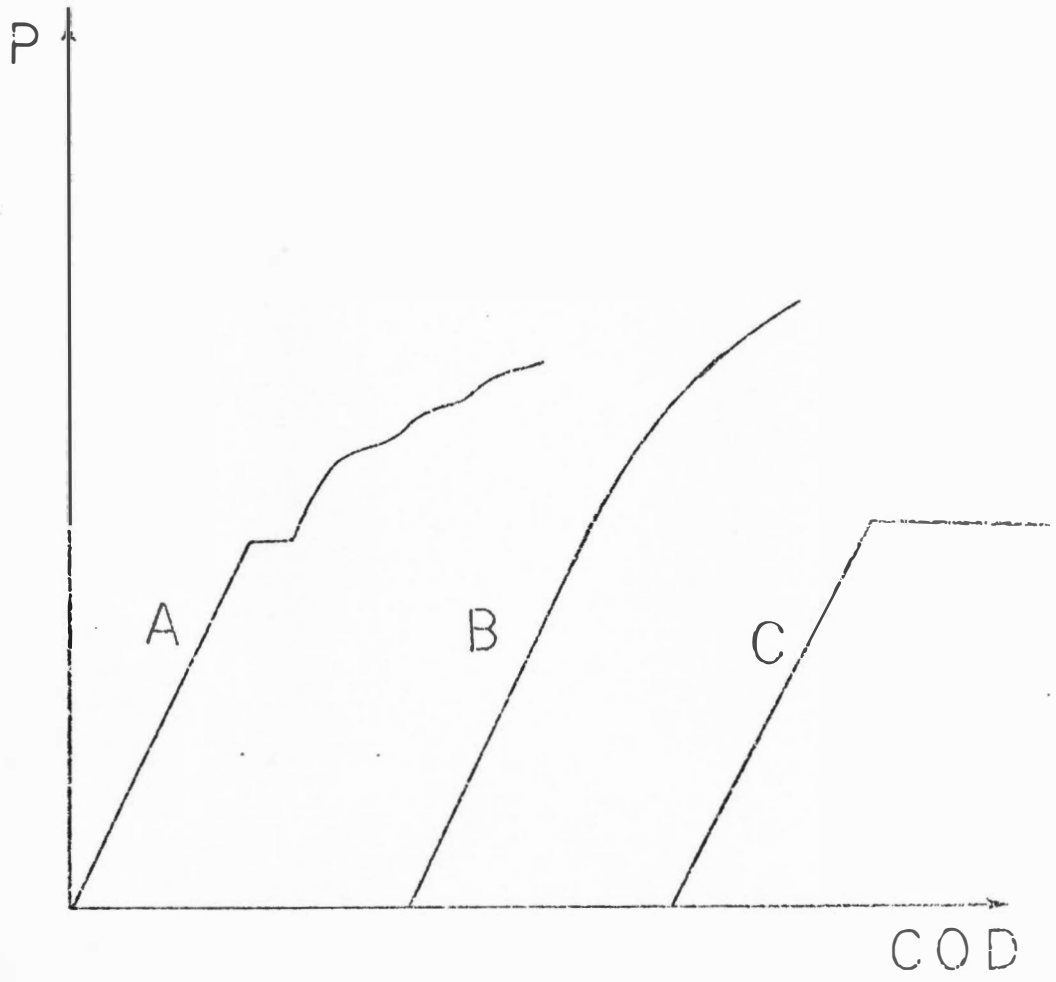

Figure 1. Typical Load-COD Curves Showing "Pop-in".

crack propagation is sufficiently small that the load instability may not be detected. In such cases, a secant modulus technique is used to calculate the presumed plane strain toughness (Figure 2).

Little attention has been directed toward determining the validity of a plane strain test based on direct evidence of brittle fracture. This is not too surprising because the test is meant to be as rapid, simple, and as inexpensive as possible, and direct observation of the fracture surface is neither rapid nor inexpensive. Nevertheless, it is unfortunate that more attention has not been devoted to the correlation of direct fracture surface evaluation by scanning electron microscopy (SEM) or replica techniques with load-COD displacement data. The validity of a plane strain test depends on whether an "inflated" value of K_{Ic} has been calculated--i.e., whether mixed mode fracture has occurred. The ductile component of the fracture would presumably increase the value of the required load at a given strain over that required for brittle fracture. The validity of a test is decided on the basis of macroscopic observations--e.g., the presence of slant fracture--or better, by conducting a series of tests with increasing plate thicknesses. The latter condition is more reasonable but offers the unattractive possibility of a large scale testing program, and/or large load capacities required for heavy section testing. Macroscopic observations to determine the validity of a test can give contradictory results, and are subject to some question. It seems somewhat questionable, for example, to inherently assume that slant fracture is produced by ductile fracture mechanisms

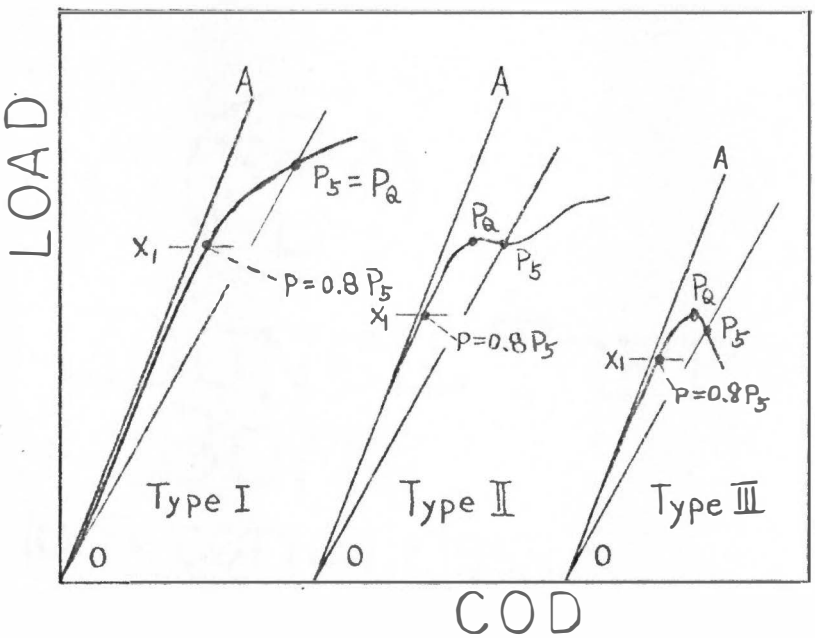

Figure 2. Load-COD Curves for Calculating Conditional Stress Intensity Factor.

and the flat fracture occurs due to the operation of brittle cleavage. The absence of ASTM procedure to determine the plane stress fracture toughness, and the previously mentioned large number of changes in the plane strain specification by ASTM, are the visible indications of the controversy and the incomplete information currently available.

The purpose of this work is to correlate SEM data of the fracture surface with load-COD data from compact tension specimens, and with the various macroscopic criteria that have been proposed, to determine the validity of a test procedure for plane strain fracture toughtness. Fracture toughness data is collected in terms of the specimen thickness, and the minimum thickness required to produce brittle fracture according to the various criteria is compared. Such a study should help to clarify the apparent anomalies between the various macroscopic criteria used to determine if a valid test has been performed.

CHAPTER II

THEORY

According to Griffith (2) who was one of the earliest workers to be concerned with failure of brittle materials, crack growth under a plane stress loading condition will occur if

$$\frac{d}{da}\left(-\frac{\sigma^2 \pi a^2}{E} + 4aT\right) = 0 \qquad (1)$$

where

$-\frac{\sigma^2 \pi a^2}{E}$ = the elastic energy loss of a plate of unit thickness under a stress, σ, measured far away from the crack, if a crack of length 2a were suddenly cut into the plate at right angles to the direction of σ.

$4aT$ = the surface energy gain of the plate due to the creation of the new surface having a surface tension, T.

This is illustrated in Figure 3 which is a schematic representation of the two energy terms and their sum to indicate a critical crack length for propagation.

When the elastic energy release outweighs the demand for surface energy for the same crack length, the crack will be unstable. One can define a gross fracture stress from this instability condition as

$$\sigma = (2ET/\pi a)^{1/2} \qquad (2)$$

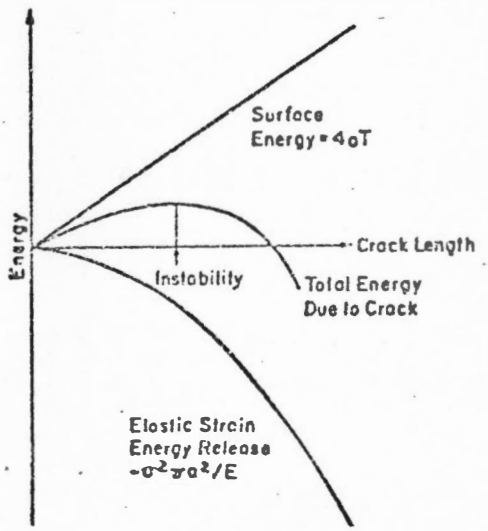

Figure 3. The Griffith Model for the Energy Balance in an Infinite Plate.

Analysis of the three dimensional problem for plane strain loading, introduces a stress in the thickness direction $\sigma_t = \nu(\sigma_\ell + \sigma_w)$, (where ν is Poission's ratio, σ_ℓ is the stress in loading direction, σ_w is the stress in the width direction), but only introduces a constant in the equations for plane stress loading. This is for plane strain condition:

$$\sigma = [2ET/(1 - \nu)^2 \pi a]^{1/2} \qquad (3)$$

In either case, the Griffith model assumes that the material in question fractures at the limit of linear elastic behavior, but does not consider the rate of crack growth. The Griffith model is limited in application, then, to those materials which are ideally brittle. Both Equation (2) and (3), which can be rewritten in the form of $\sigma(\pi a)^{1/2}$ = constant, have been shown to hold quite well for "brittle" metals, i.e., materials with negligible amount of permanent deformation preceding fracture. However, experimental work has shown that measurement of surface energy (T) is subject to much error, which in turn makes correlation of Griffith model with experimental data difficult. This has led to a search for a better model--one of which is due to Irwin (3).

Irwin applied a stress criterion instead of energy criterion for fracture and obtained:

$$\sigma_x = \frac{\sigma[\pi a]^{1/2}}{[2\pi\gamma]^{1/2}} \cos\frac{\theta}{2} \left(1 - \sin\frac{\theta}{2} \sin\frac{3\theta}{2}\right)$$

$$\sigma_y = \frac{\sigma[\pi a]^{1/2}}{[2\pi\gamma]^{1/2}} \cos\frac{\theta}{2} \left(1 + \sin\frac{\theta}{2} \sin\frac{3\theta}{2}\right)$$

$$\tau_{xy} = \frac{\sigma[\pi a]^{1/2}}{[2\pi\gamma]^{1/2}} \cos\frac{\theta}{2} \sin\frac{\theta}{2} \cos\frac{3\theta}{2} \qquad (4)$$

for a crack of length 2a subjected to a uniaxial nominal stress in the y direction. The coordinate system is shown in Figure 4.

The term, $\sigma(\pi a)^{1/2}$, which appears in both Griffith and Irwin models, has special properties--it is proportional to the stress field and reflects an equivalent between stress and the square root of crack length--and is given a special name, the stress intensity factor-K. Thus, a Griffith-type relationship results without consideration of any energy dissipation.

The fracture toughness concept can be extended one more step if a criterion for fracture is introduced. Rupture is assumed to occur at the crack tip when a critical nominal stress $\sigma = \sigma^*$ is attained at a fixed distance r*. This leads to the important result:

$$\sigma^* (\pi a)^{1/2} = K_{Ic},\ K_c = \text{constant} \qquad (5)$$

The matter of terminology is confused because McClintock and Irwin (4) define K_{Ic} as opening mode (Figure 5) fracture toughness, but do not make it clear how to distinguish between (1) plane strain versus plane stress fracture or (2) the onset of slow growth versus the onset of unstable growth. Hahn and Rosenfield (5) redefine the quantities K_c and K_{Ic} as K_{Ic} = stress intensity (value of K) at the onset of slow

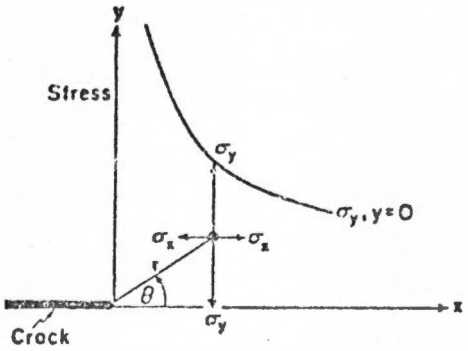

Figure 4. Schematic Illustration of the Elastic Stress Distribution Near the Tip of a Crack.

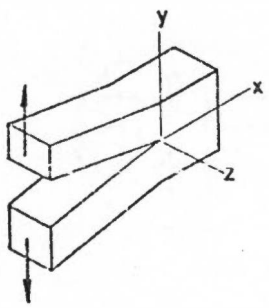

Figure 5. The Opening Mode (Mode I) of Crack Surface Displacement.

(stable) crack growth under plane strain condition. K_c = stress intensity at the onset of slow crack growth under plane stress condition.

However, for real flaws in real materials, there is no simple way to meet the rigid conditions necessary for idealized plane stress or plane strain loading, even though tentative ASTM standard laboratory procedures are available to determine K_{Ic}. This puts a severe limitation on utilizing these ASTM recommended procedures. This will be discussed in detail in Chapter IV.

Much data exist in the literature to show the transition from K_{Ic} to K_c with a decrease in specimen constraint, e.g., a decrease in specimen thickness (6, 7) (Figure 6). Accompanying this transition is the concurrent macroscopic change from flat fracture (brittle "cleavage") to slant fracture (ductile shear), and an increase in transverse strain associated with the fracture surface.

The importance of the material constants K_c and K_{Ic} is that these constants are related to basic material parameters such as σ^* and r^*, and therefore they identify the conditions for crack extension: the critical stress level and crack length. Furthermore, K_{Ic} defines the minimum energy to cause initiation (and propagation) of the crack.

In both the Griffith and the Irwin theories discussed above the material is assumed to be linearly elastic and therefore ideally brittle. In real materials, particularly medium and low strength materials, there is often plastic flow adjacent to the tip of the advancing crack, introducing one more experimental parameter to be

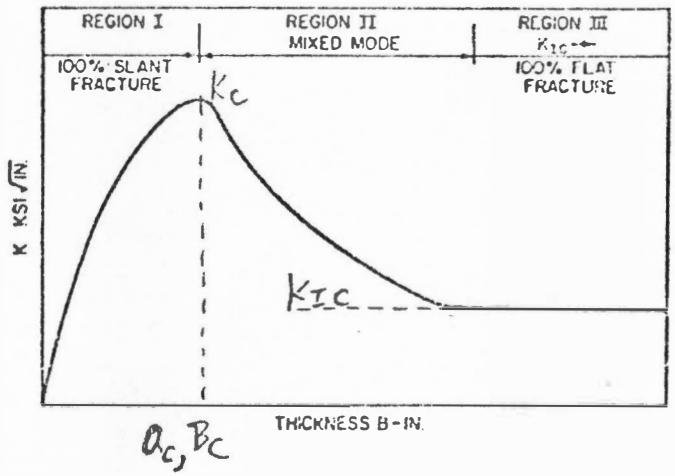

Figure 6. Influence of Specimen Thickness (B) and Crack Length (a) on Fracture Toughness (K).

considered in determination of K and making the validity of the Griffith and the Irwin models suspect. A plastic zone correction factor, r_p, can be estimated from Equation (4) by setting $\sigma_y = \sigma_{ys}$, the nominal yield strength of the material, which results in

$$r_p = \frac{1}{2\pi}\left(\frac{K}{\sigma_{ys}}\right)^2 \qquad \text{plane stress}$$

$$r_p = \frac{1}{6\pi}\left(\frac{K}{\sigma_{ys}}\right)^2 \qquad \text{plane strain} \qquad (6)$$

This correction factor has been successfully applied in cases where only a small amount of plastic deformation occurs, and where that plastic deformation occurs prior to crack growth.

From a toughness viewpoint, local plastic flow in front of the advancing crack tip may well be desirable. If flow occurs, elongation in the load direction occurs, which results in "blunting" of the crack tip (Figure 7). This in turn increases the stress required to cause continued crack propagation.

Plastic flow in front of the crack tip absorbs stored elastic strain energy decreasing the amount of stored energy available to create new crack surface. In addition, plastic flow in the load direction increases the radius of the crack tip which decreases the stress concentration factor, which decreases $K_{applied}$, which may cause $K_{applied}$ to be less than K_c, causing cessation of crack growth (8). For this reason, the stress field with plastic flow is changed from Figure 4 to Figure 8. Adjustment of K values was made by substituting

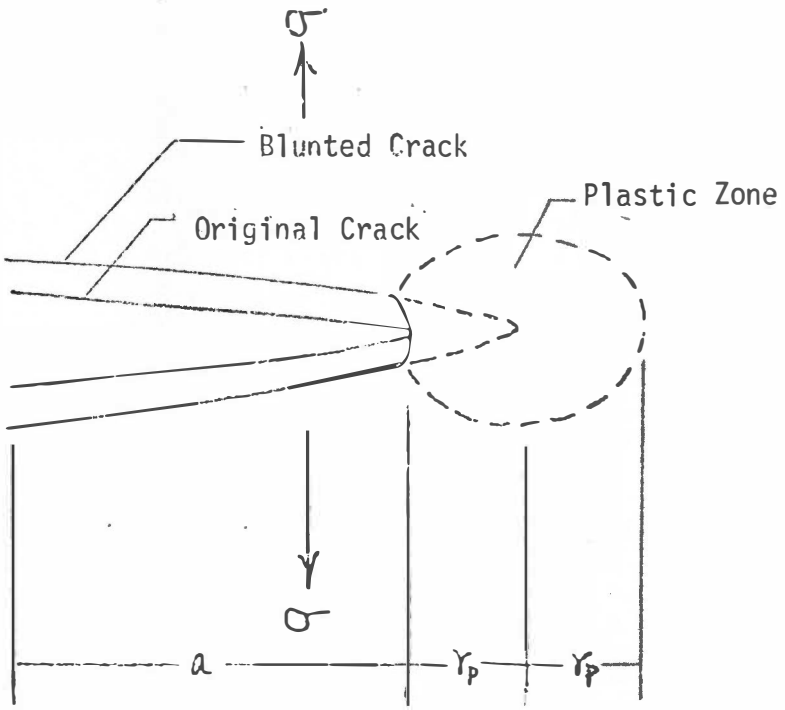

Figure 7. Schematic Indication of Crack Blunting Due to Extension in the Load Direction.

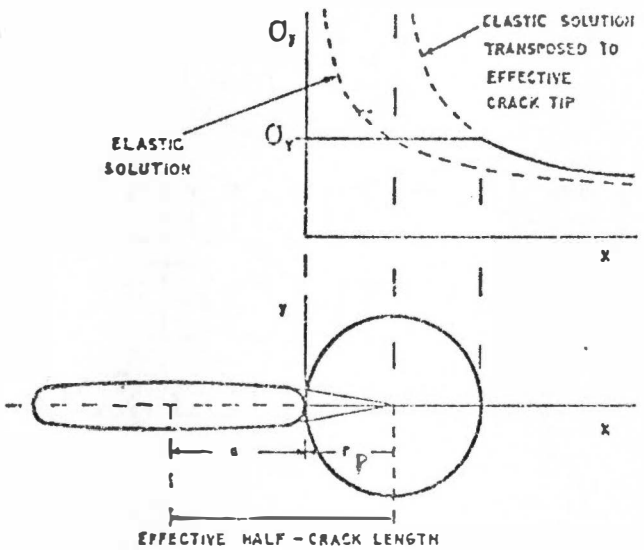

Figure 8. Increase in Effective Crack Length Due to Plastic Zone Formation at the Crack Tip.

the effective crack length $2(a + r_p)$ for the actual crack length.

In considering the change of the plastic zone sizes, it is reported (5) that for materials which have a low strain hardening coefficient (n), the shape of the plastic zone is planar, but if (n) increases, the zone will expand in the loading direction (Figure 9). The plastic zones have been observed to change in the same way if specimen constraint changes loading the condition from plane stress to plane strain. Therefore, both metallurgical and geometrical factors are involved in defining the amount of plastic flow associated with or prior to crack growth.

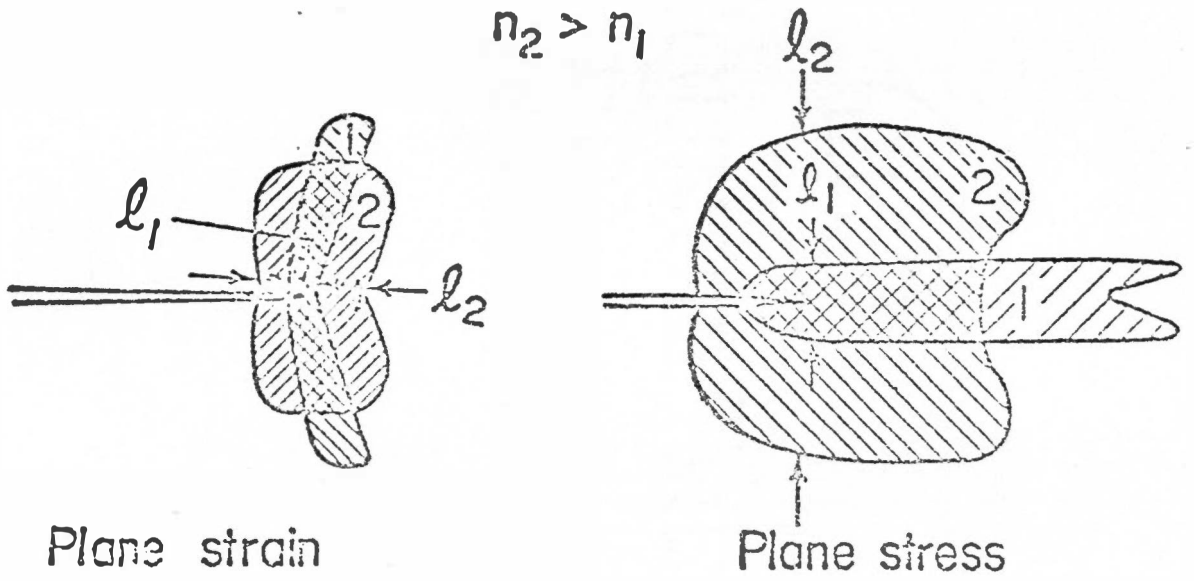

Figure 9. Influence of the Strain Hardening Coefficient on Plastic Zone Shape.

CHAPTER III

EXPERIMENTAL PROCEDURE

Materials

The material used for this investigation was an O1 tool steel, heat treated to a low hardness. Chemical composition of this material is listed in Table 1, and mechanical properties determined from tensile specimens are listed in Table 2. Metallographic examination and SEM microscopy show that the microstructure consists primarily of a dispersion of carbide particles in a ferrite matrix (Figures 10, 11) which is characteristic of either the annealed or quenched and tempered condition. Some patches of pearlite were detected (Figure 11) which indicate that the material was probably in the annealed condition.

Test Specimens

Fracture toughness compact tension specimens were fabricated based on ASTM Standard E-399 (Figure 12) (9). One inch thick specimens were made according to this specification. Thinner specimens were made such that all dimensions were identical to the one inch thick specimen except the thickness, e.g., crack length, loading pin location. A total of seven different thicknesses were prepared, varying from 0.125 to 1.00 inches. (Preliminary testing of the compact tension specimens indicated that the 1.00 inch thickness was near the maximum that could be fractured using the available Instron loading frame.)

TABLE I

CHEMICAL COMPOSITION & HEAT TREATMENT

Chemical Composition (Weight Percent)	Heat Treatment
0.9 C, 1.3 Mn 0.5 W, 0.5 Cr	Harden at 1475°F, and tempered at 450°F, or annealed at 1450°F, as received

TABLE II

MECHANICAL PROPERTIES

Yield Strength (0.2%)	55,500 psi
Utimate Strength	101,000 psi
Tensile Elongation	25%
Reduction in Area	50%
Hardness	R_C 10
Strain Hardening Coefficient	0.233

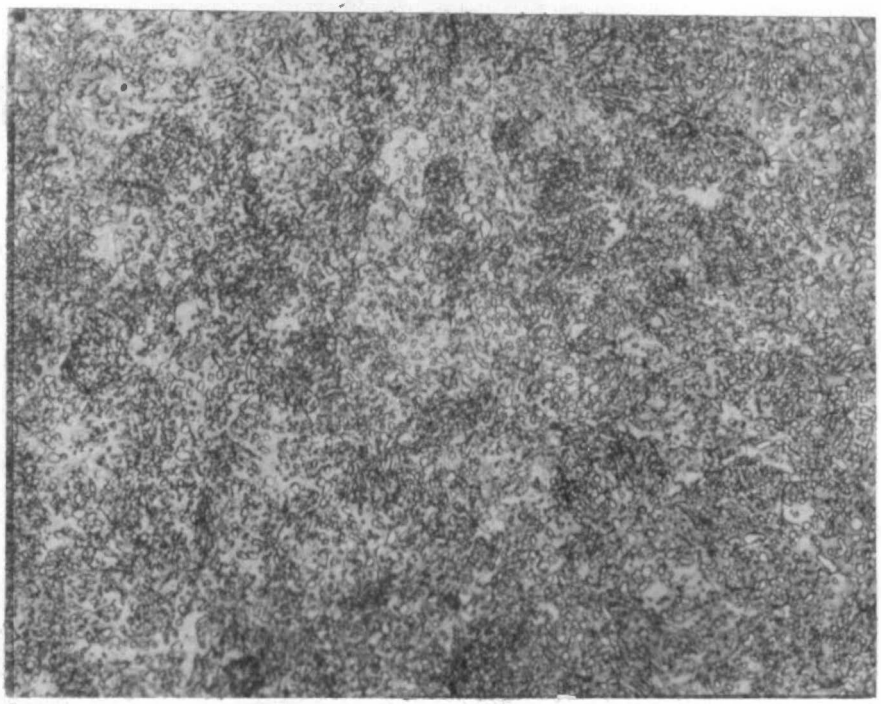

Figure 10. Optical Micrograph of the Etched Plan View of the Compact Tension Specimen After Loading to 90% of the Fracture Load. Mag.: 750X.

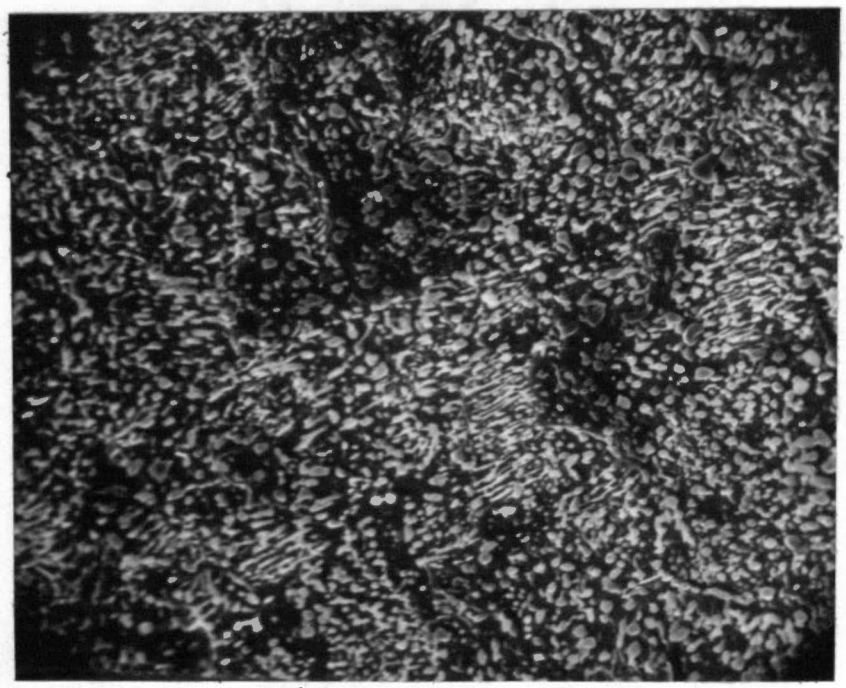

Figure 11. SEM Micrograph of the Same Surface as Figure 10. Mag.: 2000X.

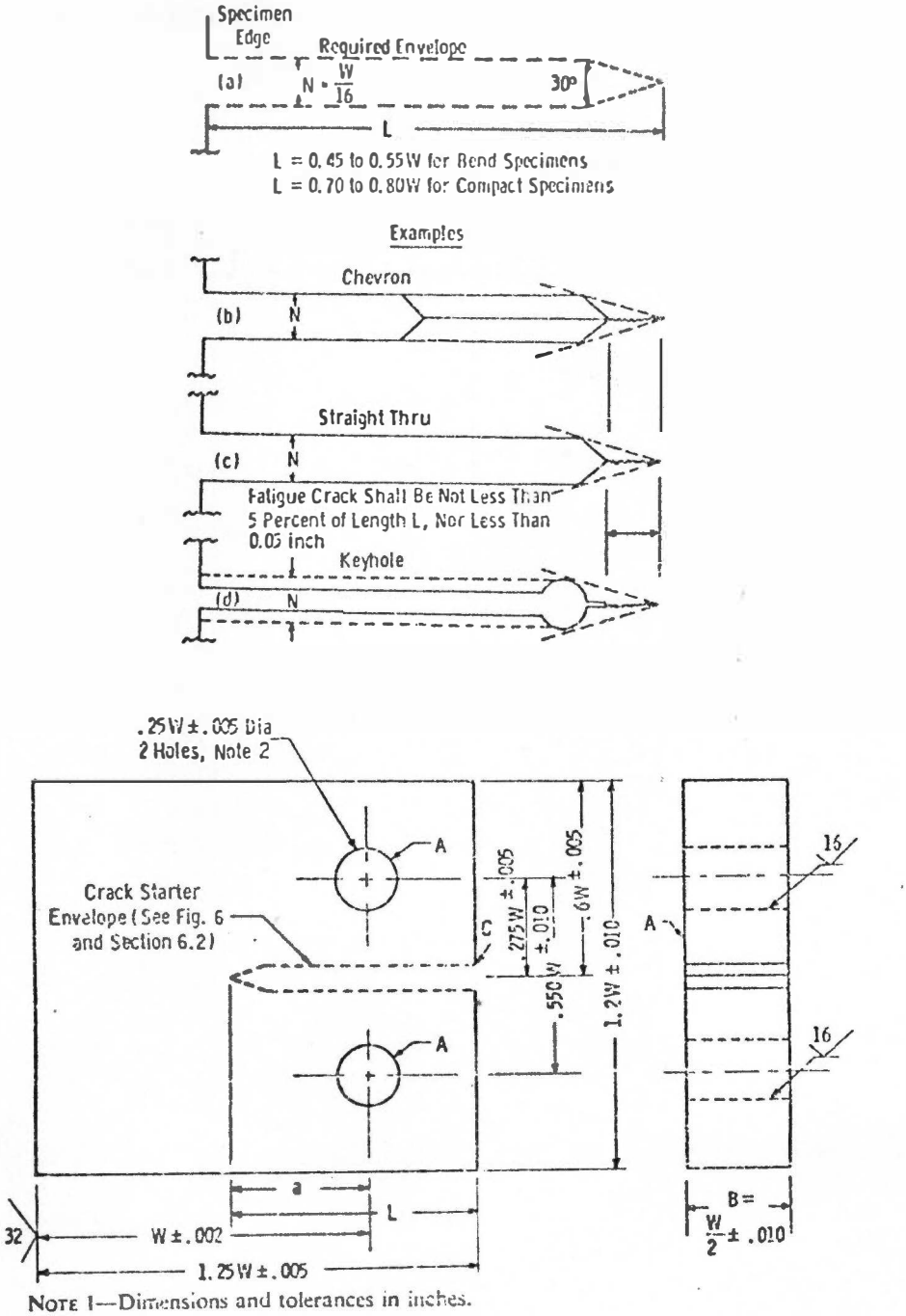

NOTE 1—Dimensions and tolerances in inches.

Figure 12. Compact Tension Specimen Geometry and Crack Starter Envelope Geometry.

The notch tip radius of the specimens was estimated to be about 0.003 inches (based on metallorgaphic examination).

Tensile Loading

Specimens were loaded in an Instron Universal Testing Machine having a maximum load capacity of 20,000 pounds. A crack opening displacement gage (COD) was fabricated according to ASTM E-399 standards, and which utilized four averaging strain gages to monitor the opening of the crack during loading (Figure 13). Load-COD data was simultaneously monitored using the Instron x-y recorder. Tests were conducted at a constant crosshead velocity of 0.02 inches/minute at room temperature.

At least two specimens were tested at each thickness. For a given thickness, one specimen was loaded to failure in order to obtain load and displacement data to calculate fracture toughness and to provide specimens for SEM evaluation of the fracture surface. The second specimen was then loaded to 90 percent of the maximum load of the broken specimen in order to measure the size and shape of the plastic hinge at the notch tip, and to measure the transverse (i.e., thickness) strain at the notch tip. Some duplicate specimens were run for data points that initially did not lie on a smooth curve of the maximum load versus specimen thickness.

Specimens were prepared such that the rolling plane was the specimen plan view and the load was applied perpendicular to the rolling direction (Figure 14).

In the initial stage of the work an attempt was made to utilize

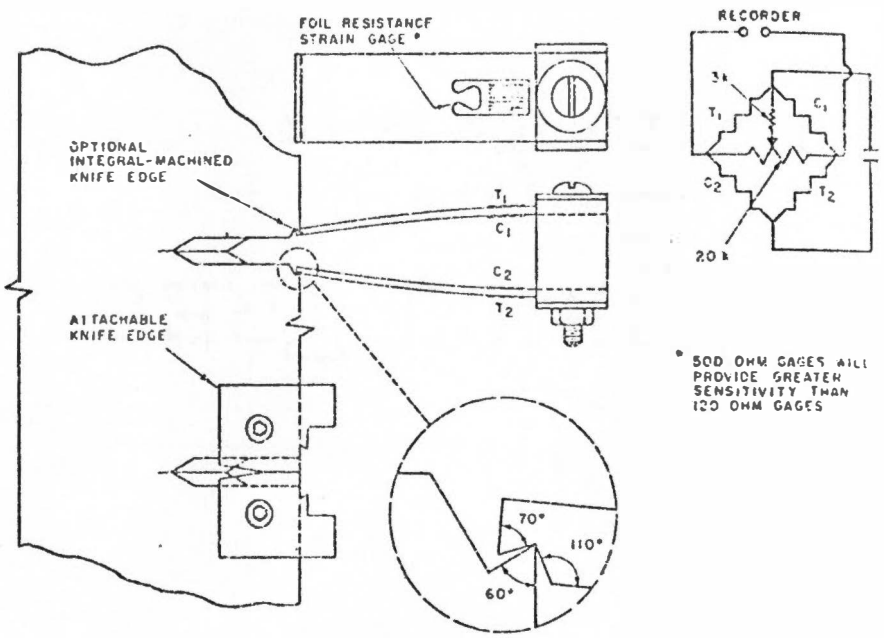

Figure 13. Averaging COD Displacement Strain Gage and Mounting Method for the Gage.

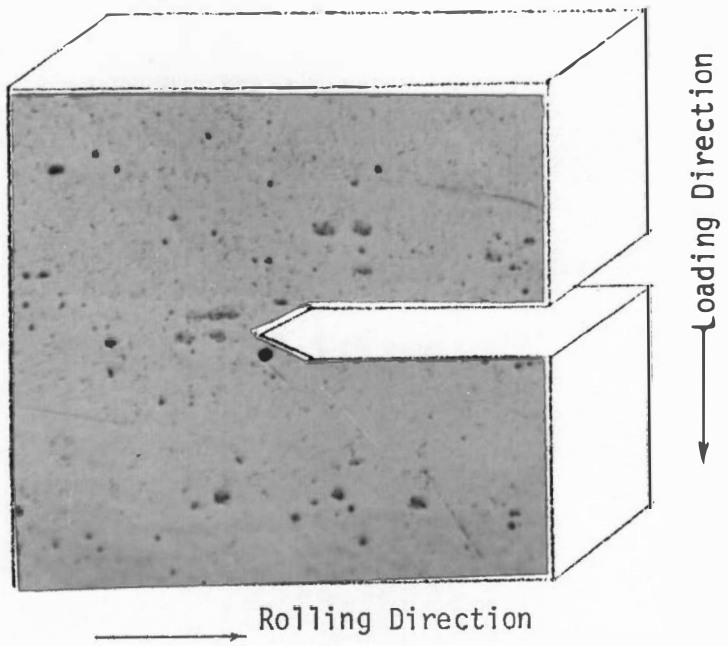

Figure 14. Orientation of the Loading Direction with Respect to the Rolling Direction of the Plate.

microhardness measurements to define the plastic zone shape and the strain gradient within the zone. Microhardness measurements also allow plastic zone sizes to be determined below the surface of the specimen. Since thicknesses were choosen so as to cover the brittle to ductile fracture region, knowledge of the subsurface plastic strain gradient was considered desirable. However, preliminary results using indentor loads as low as ten grams were unable to give a clear picture of either the size of the zone or the strain gradient within the zone. This was felt to be at least partially due to the magnitude of the strain hardening coefficient for this material. Other author (10) has used the low load microhardness measurements to define plastic zones in front of growing cracks with some success. Additionally, the size of the plastic zone was sufficiently small due to the geometrical constraint that even at the lowest indentor loads it was impossible to obtain a sufficient number of reading within the zone to define the strain gradient in the thicker specimens.

Since it was still considered necessary to have some indication of the hinge zone on the side of the specimen, a metallographic technique was developed which unfortunately would reveal only the size of the hinge zone and not the strain gradient within the hinges. This additionally precluded determination of the hinge zone below the specimen surface. As will be seen in the discussion, it would have been desirable to have this information. The hinge zone was revealed by metallographically polishing the test specimen prior to loading, and after loading to rub the specimen across 3/0 emergy

paper (Figures 15, 16).

Scanning Electron Microscopy

The SEM is the ideal tool to use for the fractography because of the large depth of the field available in SEM microscopy. Additionally, direct examination of the sample including the rough surface is possible. SEM was performed using an AMR-900 scanning electron microscope in order to observe changes in fracture mechanisms with specimen thickness.

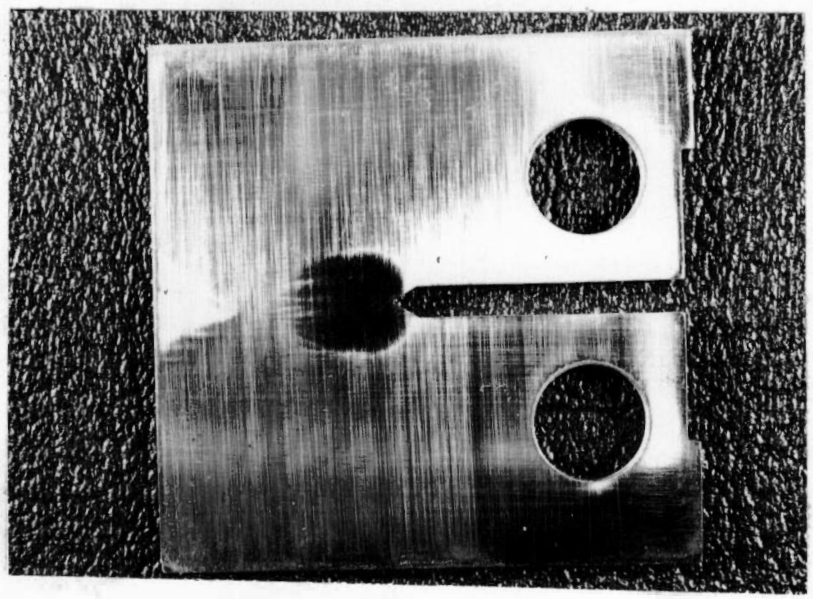

Figure 15. Surface Polished 0.125 Inch Thick Specimen Showing Surface Plastic Zone Formation.

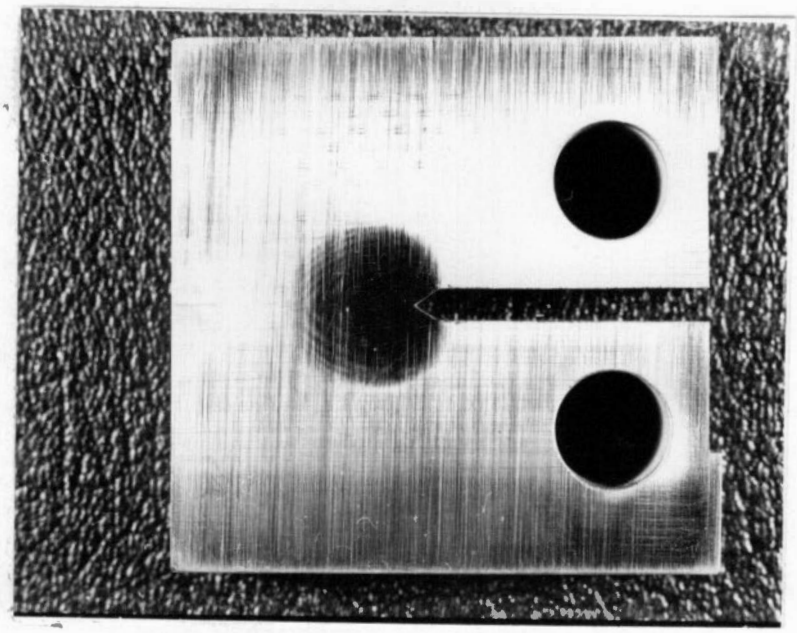

Figure 16, Surface Polished 0.477 Inch Thick Specimen Showing Surface Plastic Zone Formation.

CHAPTER IV

RESULTS AND DISCUSSION

Introduction

In order to draw conclusions with respect to the micro and macroscopic transitions of ductile-brittle behavior with thickness, all load and displacement data were plotted in terms of the thickness parameter. Initially, the experimental load-COD curves are discussed in terms of the observed proportional (P_p) and maximum (P_m) loads. The second section of the discussion compares observed strain measurements with SEM results. This section contains remarks about the gross plastic flow in terms of the number of chevron shaped crack arrest zones observed on the fracture surface, shear lip area, lateral contraction, and the correlation of these observations with SEM microscopy. Finally, the last portion of the discussion considers the implications derived from this study regarding ASTM E-399 requirements to calculate a valid K_{Ic} from load-COD data. It is hoped that because of these results, a better knowledge of fracture behavior can be obtained.

Load-COD Data

Figure 17 shows the change in the observed maximum load (P_m), the proportional load (P_p), and the secant modulus intercept load (P_Q) used to calculate the fracture toughness as specimen thickness is increased. (P_Q is the load intercept for a secant line having a

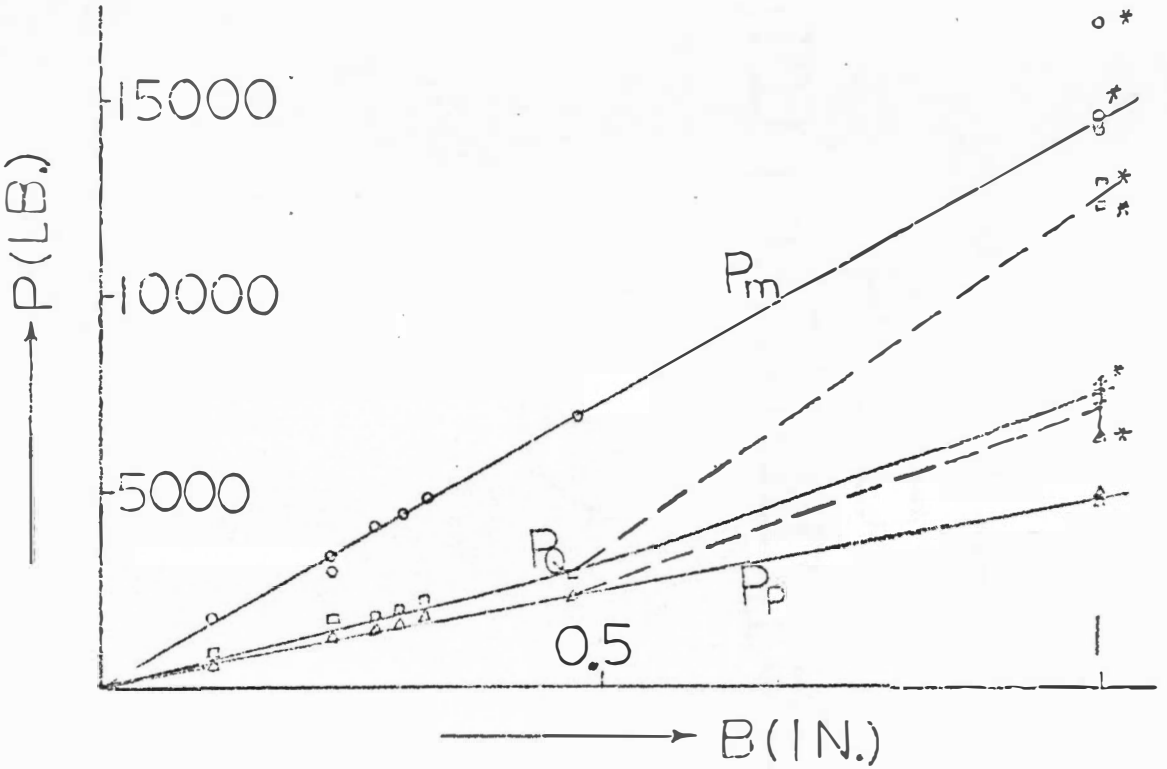

Figure 17. Proportional Load (P_p), Secant Intercept Load (P_Q), and Maximum Load (P_m) as a Function of Specimen Thickness.

slope five percent less than the linear portion of the load-COD curve.) It is noticed that both P_m and P_p increase linearly with thickness in spite of increasing constraint. P_Q, however, increases nonlinearly with thickness. Data are also plotted in Figure 18 as the ratios P_p/P_m and P_Q/P_m. These plots indicate that the ratio P_Q/P_m increases with thickness but that P_p/P_m does not change with thickness, at least for thicknesses greater than 0.232 inches. The low value of P_p/P_m (about 0.32) might well incorrectly be taken to indicate a "ductile" material, or the lack of sufficient constrain to cause plane strain fracture. There is some indication that P_p/P_m might decrease for thinner specimens.

The increase of P_Q/P_m with thickness is expected since constraint is increased as thickness is increased. That is, the loading more closely approaches the plane strain condition. The constancy of the ratio P_p/P_m was not expected.

If load data are normalized with respect to the thickness and replotted against COD displacement (Figure 19), these data indicate that both P_m/B and P_p/B remain constant, but that P_Q/B still increases with thickness. The constancy of P_p/B with thickness may be an indication of crack initiation. If it is assumed that plastic flow occurs in front of the notch tip, one would expect the effective stress to be reduced as the thickness is increased. This implies that flow will initiate at larger and larger values of the nominal stress. (P/B is directly equivalent to the nominal stress since the width dimension is constant for all specimens.) If, on the other hand,

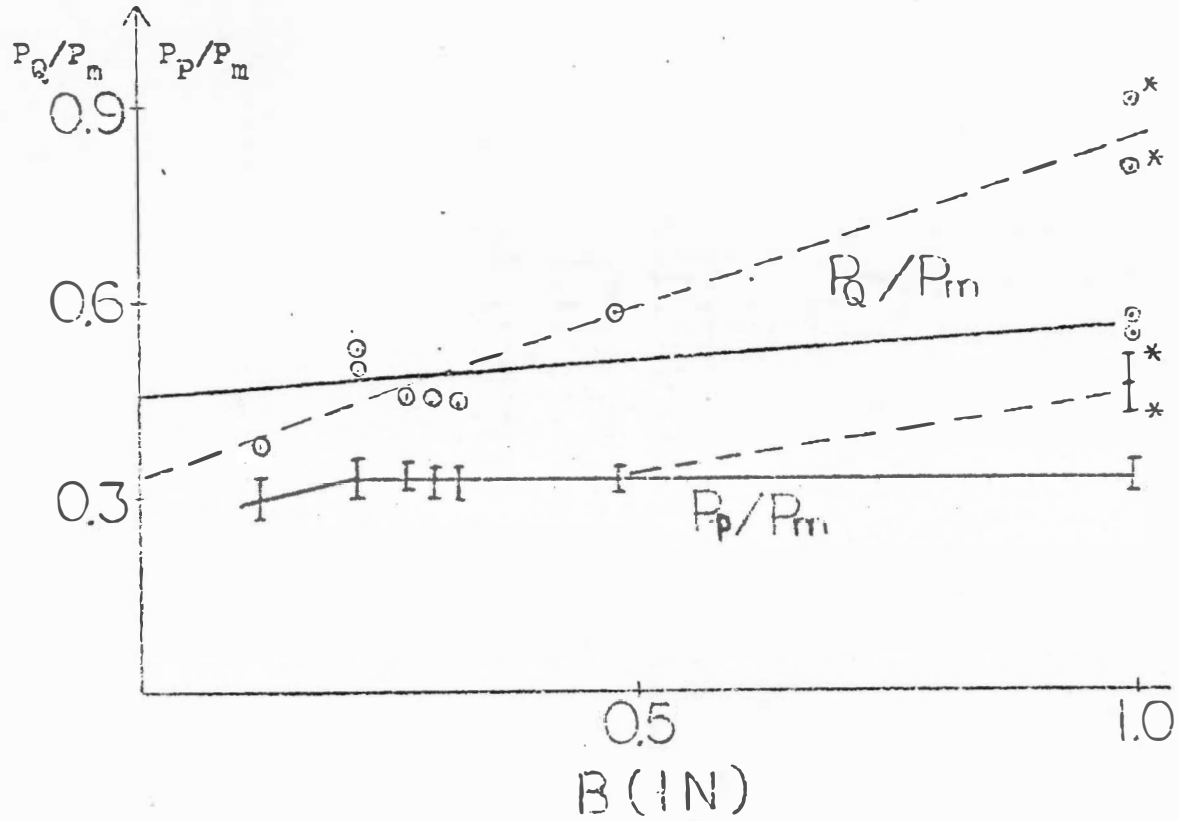

Figure 18. The Ratios P_Q/P_m and P_p/P_m as a Function of Specimen Thickness.

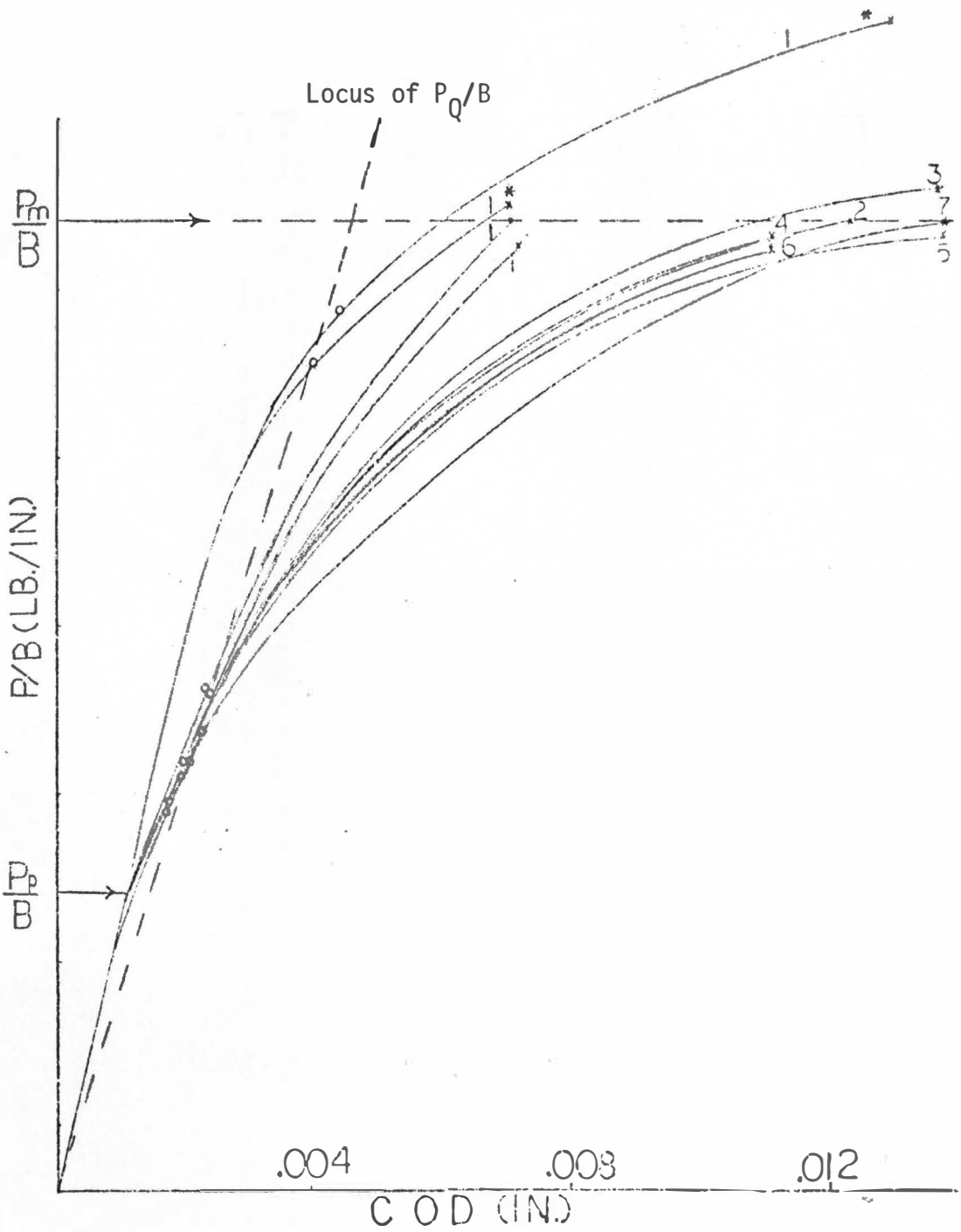

Figure 19. Normalized Load (P/B) as a Function of COD Displacement, Where 1 Indicates 1.00 inch Specimen, 2 Indicates 0.477 Inch, 3 Indicates 0.330 Inch, 4 Indicates 0.300 Inch, 5 Indicates 0.275 Inch, 6 Indicates 0.232 Inch, 7 Indicates 0.125 Inch, and * Indicates pop-in.

sufficient constrain exists to cause the normal stress on the crack plane to become equal to the crack initiation stress, prior to or simultaneously with the approach of the effective stress to the flow stress, then P_p/B is in fact a measure of the crack initiation stress. Equation (4) for the normal stress acting on the fracture plane shows that the normal component of the stress acting at the crack front depends on crack length, notch radius, and nominal stress. That is, the normal stress on the fracture plane does not depend on constraint in the specimen, but does depend directly on the nominal stress. Now the maximum nominal stress that can be applied to a material is the "breaking stress," so that if sufficient constraint is present, the applied load reaches the value of the crack initiation normal stress before it reaches the value of the effective stress required to cause plastic flow. The resulting implication is that this condition exists for specimens 0.232 inches thick and thicker, and that the proportional limit corresponds to crack initiation. The crack initiation stress does not vary with thickness once a critical amount of constraint is achieved if there is no prior plastic flow, or if crack initiation is by a ductile mechanism. SEM data, however, indicate that the plastic initiation hinge zone (PIZ) is created by a ductile mechanism. This would imply that P_p/B should increase with thickness. Consequently, this dilemma must remain unresolved.

Gross Plastic Flow and SEM Microscopy

For the purposes of analysis, it is helpful if the trends in the

observed results with an increase in specimen thickness are listed:

1. A decrease in the relative amount of ductile to brittle fracture as determined by either macroscopic or microscopic techniques. For example, Figure 20 shows that the ductile area of the fracture surface, based on macrophotographic evidence, decreases from 33.5 percent for the 0.125 inch specimen to 2.2 percent for the 1.000 specimen. Figure 21 shows the appearance of the macroscopic fracture surfaces and illustrates the appearance of the ductile and brittle portions of the fracture surface including the chevron chaped crack arrest zones.

2. A decrease in the ratio of shear lip to total fracture area (Figure 22). The shear lip area decreases exponentially up to a thickness of about 0.5 inches and then remains constant.

3. An exponential decrease in the amount of lateral contraction as measured by a point micrometer. Lateral contraction in the 0.125 inch thick specimen is about 9.5 percent and decreases to 0.77 percent in the 1.00 inch specimen (Figure 23). (Note that the reduction in area observed in the unnotched tensile specimens was 50 percent.)

4. A decrease in the length and an increase in the height of the plastic zone on the plan view of the specimen (Figure 24).

Items (1), (2), and (3) clearly show the transition from ductile or mixed mode to brittle behavior as constraint is increased. Item (4) is considered to be evidence of a transition from plane stress to plane strain loading (5). Considering these four observations, the

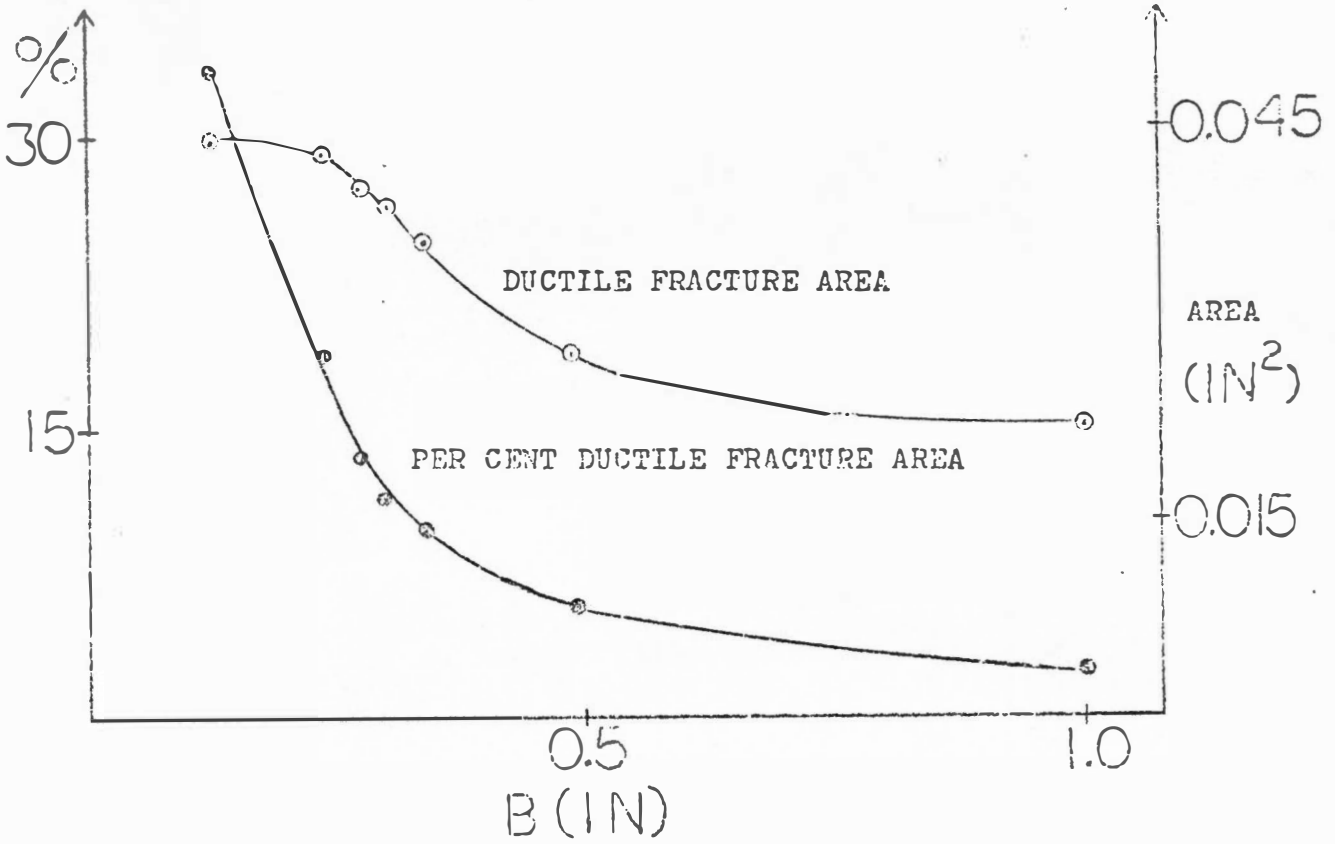

Figure 20. Ductile Fracture Area and Percent Ductile Fracture as a Function of Specimen Thickness, Based on Macroscopic Appearance.

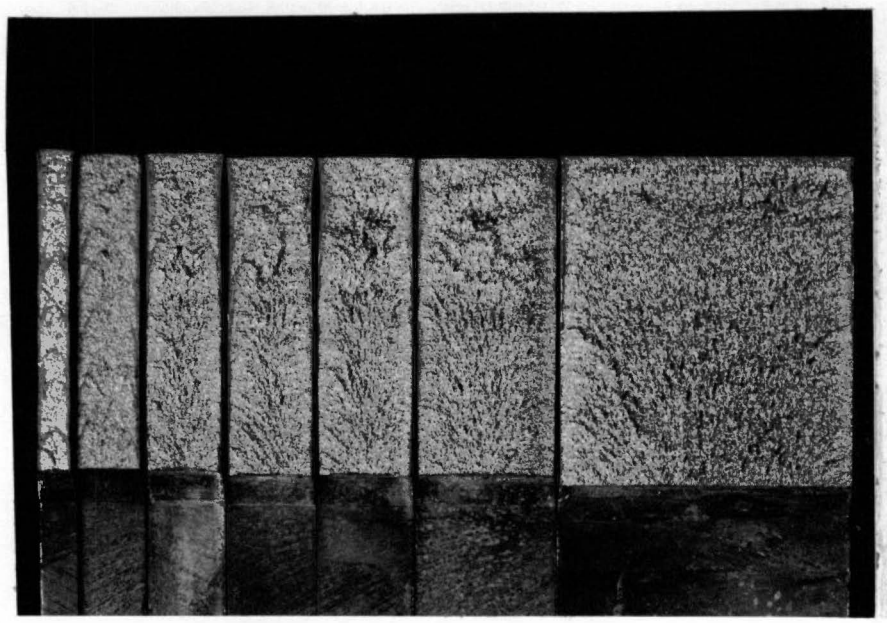

Figure 21. Fracture Surface Appearance as a Function of Specimen Thickness.

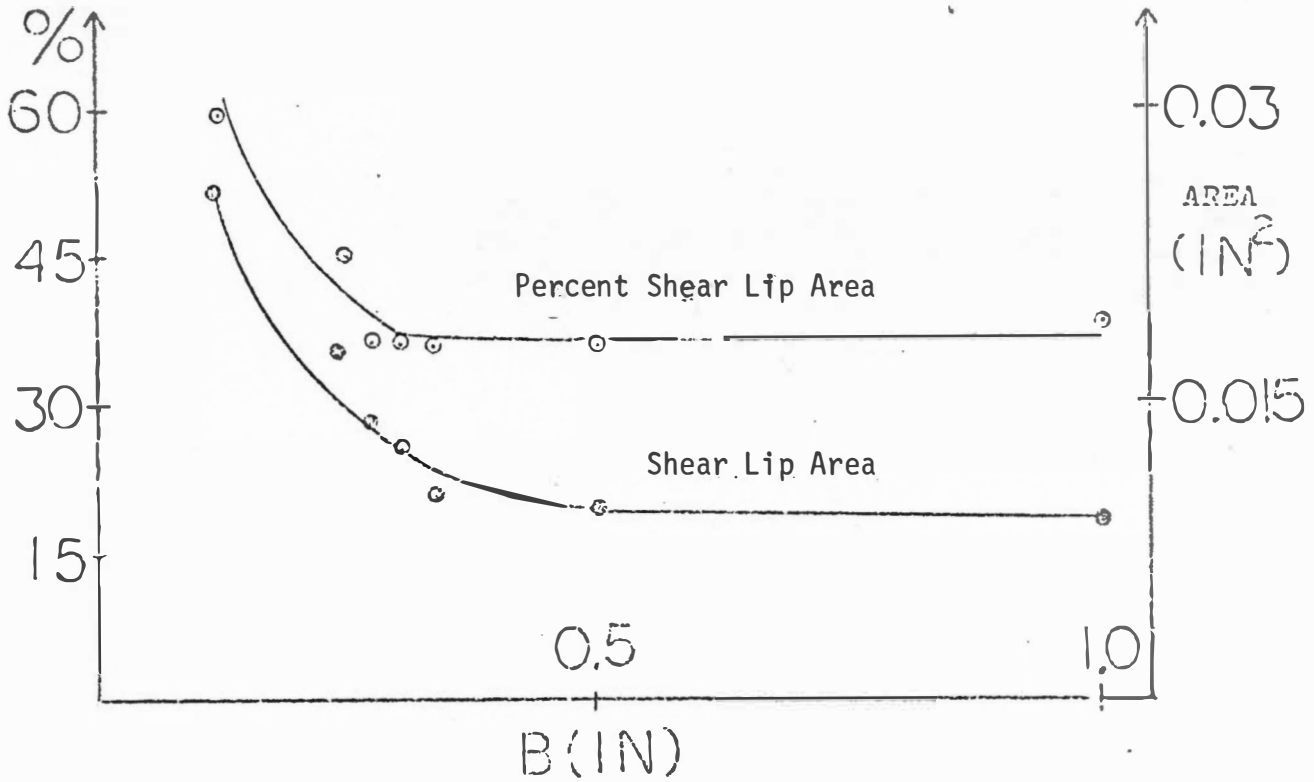

Figure 22. Shear Lip Area and Fraction of Shear Lip Area of the Total Ductile Fracture Area as a Function of Specimen Thickness.

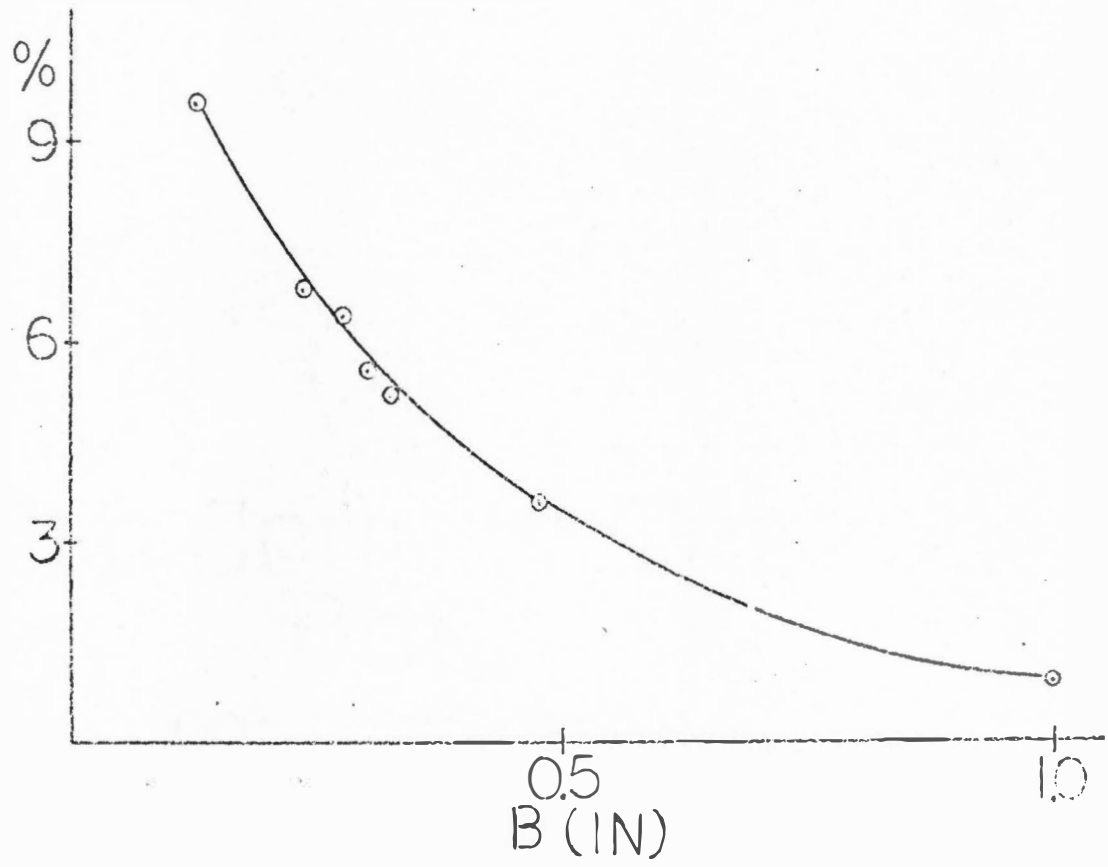

Figure 23. Percent Lateral Contraction as a Function of Specimen Thickness.

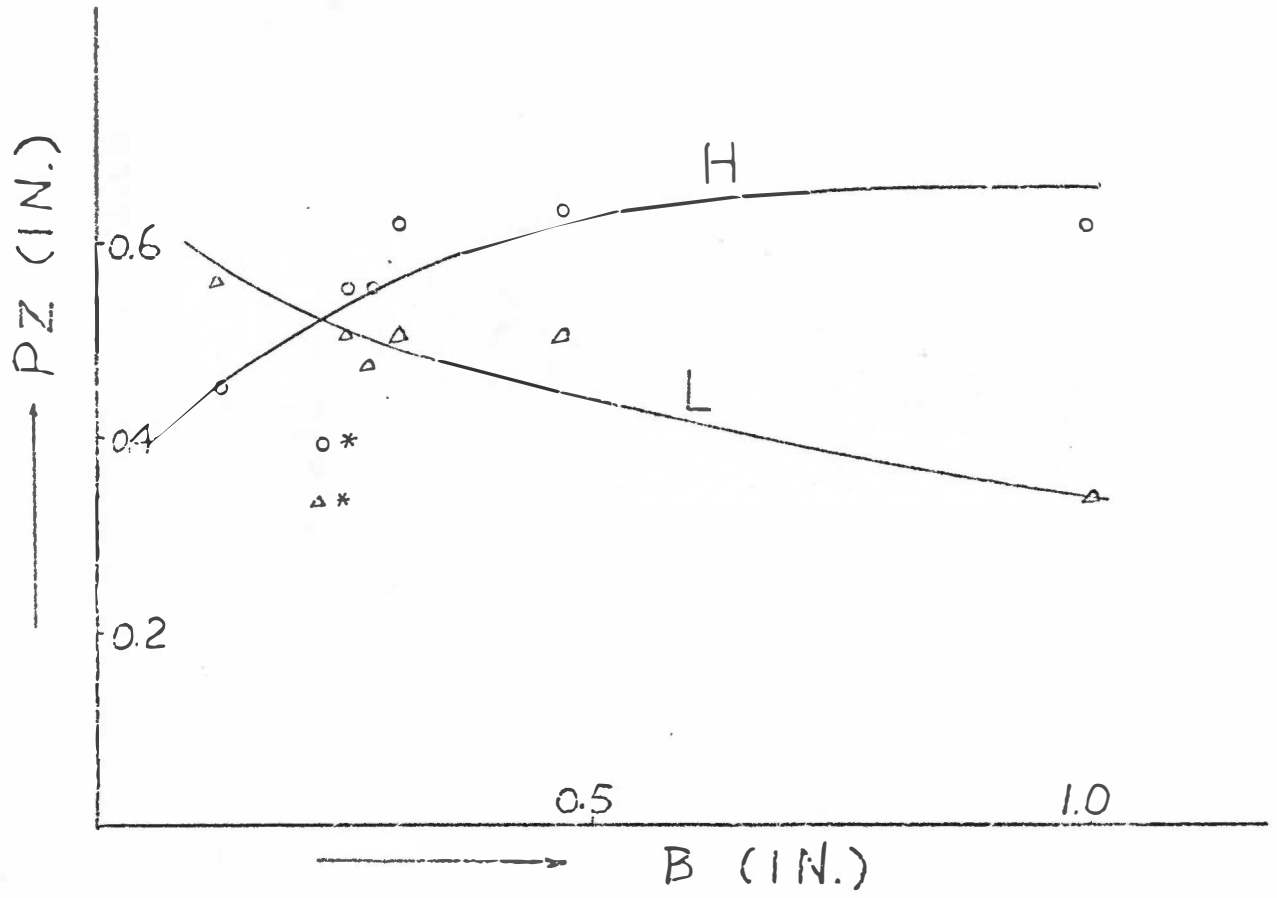

Figure 24. Length (L) and Height (H) of the Plastic Zone on the Plan View of the Compact Tension Specimen as a Function of Specimen Thickness. (*The Two Data Points at 0.232 Were for Specimens Probably Loaded to Less than 90% of the Fracture Load.)

conclusion may be drawn that the transition from ductile to brittle behavior from a macroscopic point of view is equivalent to the transition from plane stress to plane strain behavior.

Figure 25 shows the chevron shaped arrest zones that were observed in the thinner specimens. These zones are assumed to indicate a transition from microscopic brittle to ductile behavior. Figure 26 shows the number of chevron arrests decrease as the thickness is increased. The fractograph for the 0.232 inch specimen (Figures 27, 28) show that crack propagation involves void generation around the carbide particles presumably in front of the growing crack front.

For thin specimens, shear on planes inclined 45° to the load axis can penetrate through the thickness as well as along the width direction (Figure 29). This form of relaxation cannot support a stress normal to the specimen surface. Thus, the peak stress in this region cannot be greater than the flow stress. As the load is increased to a value that creates a local stress equal to the critical stress for crack initiation, the brittle crack forms and starts to propagate. Since the elastic strain energy used in the creation of the plastic zone is a large fraction of the total stored elastic strain energy (Figure 30), little energy is available to propagate the crack and arrest soon occurs. Since the strain energy remaining in the specimen after each arrest is less than that at the prior arrest, the distance between arrest zones decreases as the crack propagates across the width of the specimen.

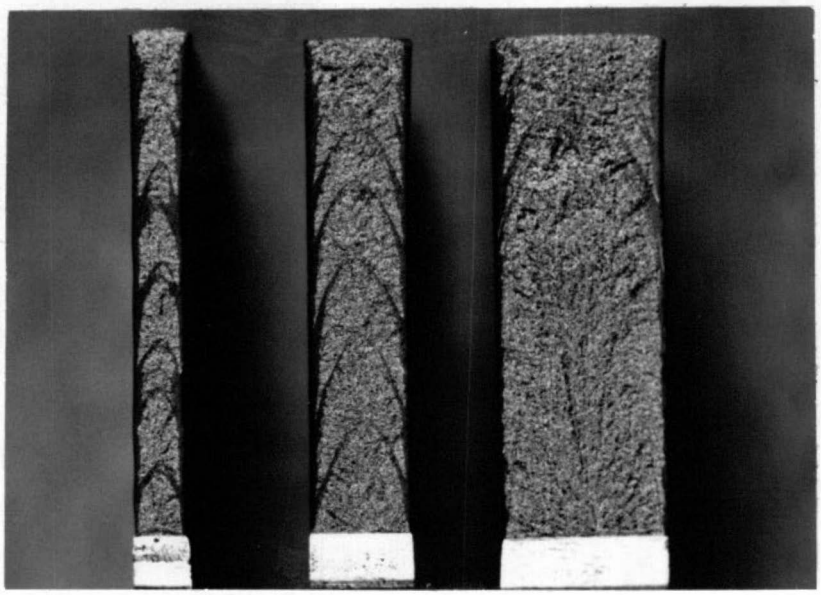

Figure 25. Fracture Surface of the 0.125, 0.232, and 0.330 Inch Thick Specimens Showing the Presence of Shear Lips and Fracture Arrest Zones.

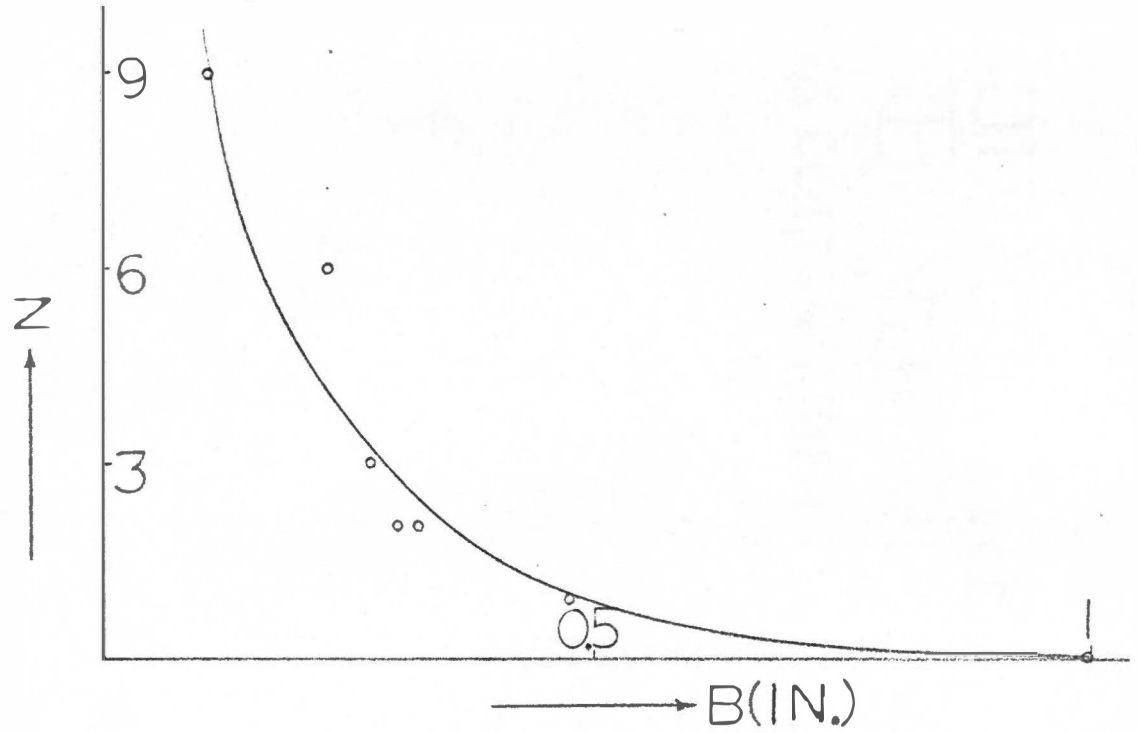

Figure 26. Number of Chevron Arrest Zones as a Function of Specimen Thickness.

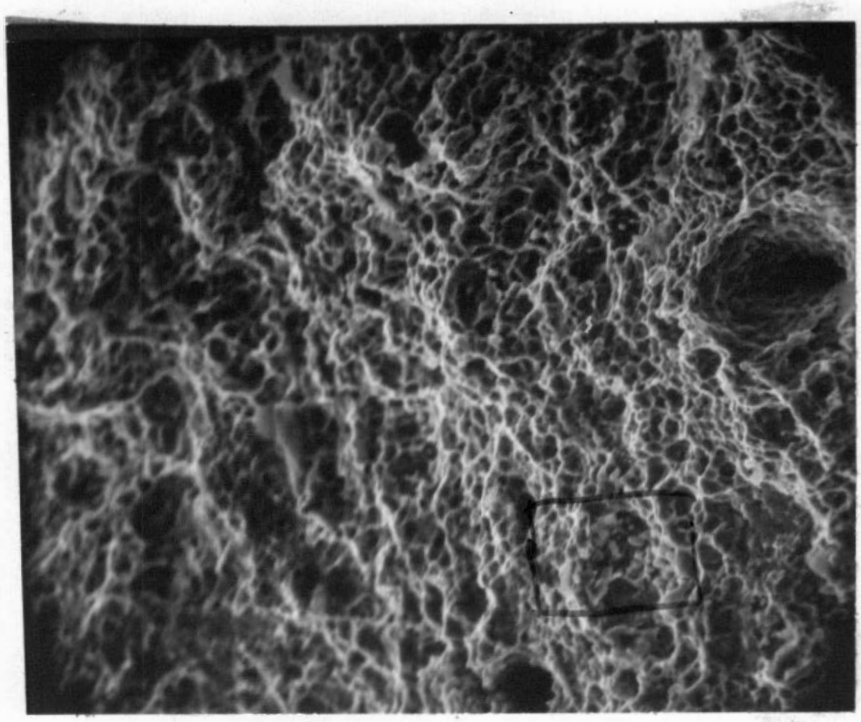

Figure 27. SEM Fractograph of the 0.232 Inch Specimen. Area Shows Plastic Dimpled Fracture. Mag.: 1600X.

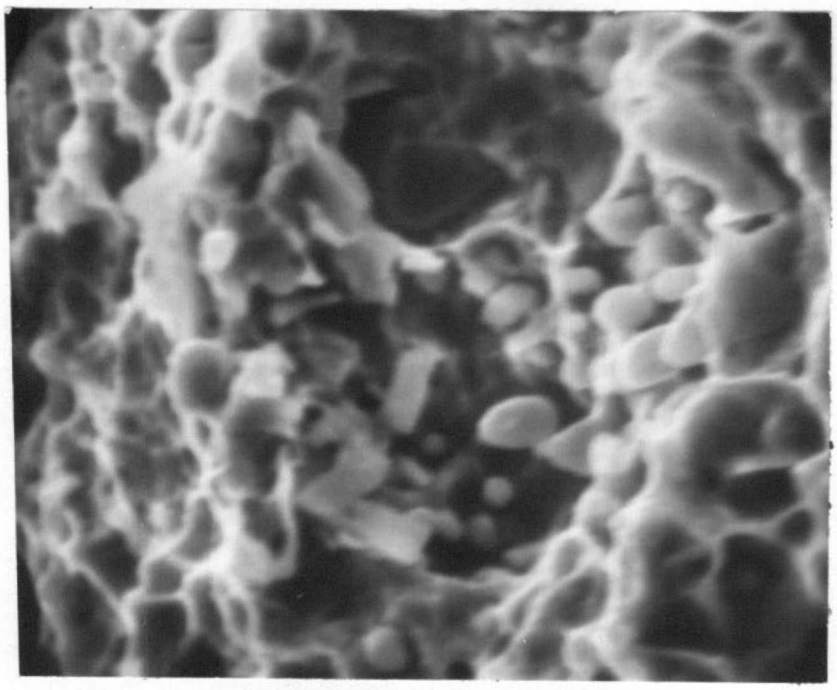

Figure 28. SEM Fractograph of the Indicated Region in Figure 27. Area Shows Carbide Particles Inside Voids. Mag.: 8000X.

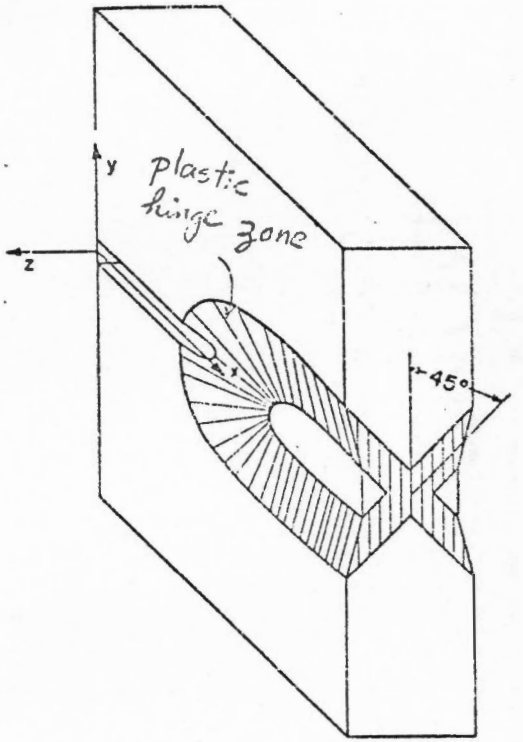

Figure 29. Schematic Illustration Showing Shear Stress Inclined 45 Degrees Penetrated Through the Thickness.

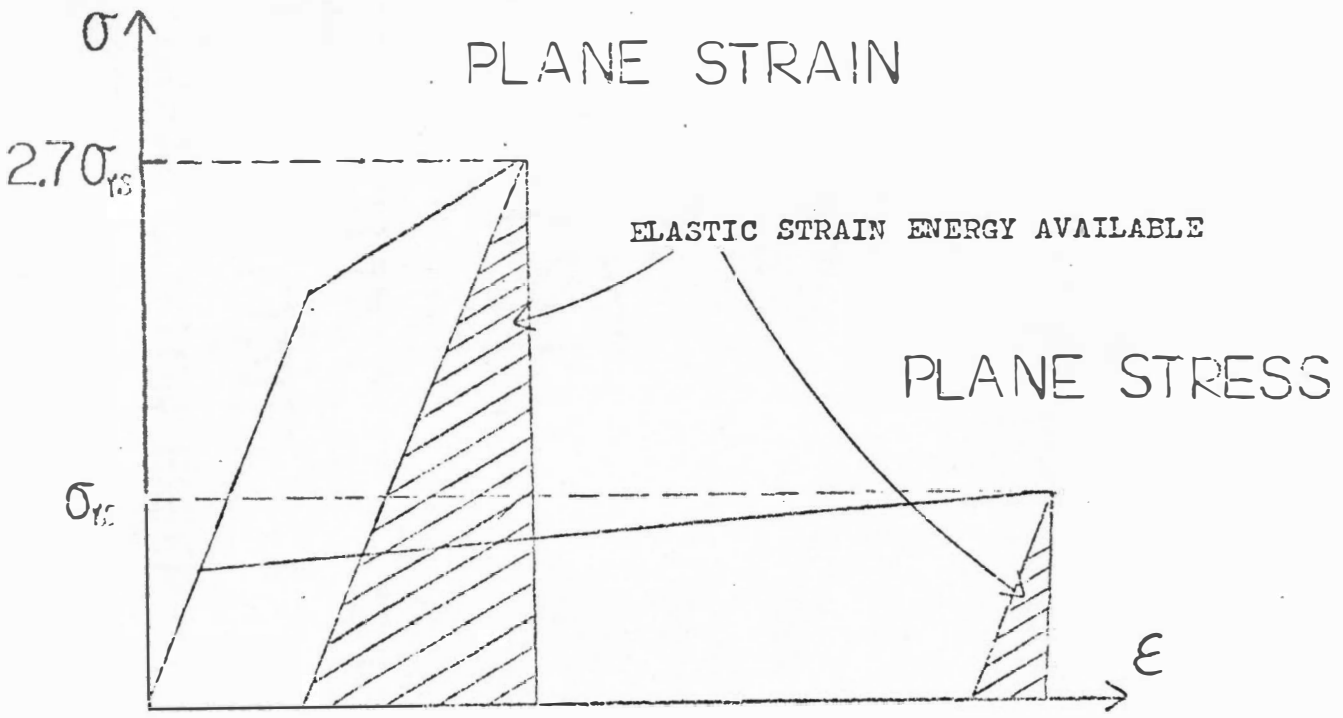

Figure 30. Postulated Idealized Stress-Strain Curves for Plane Stress and Plane Strain Loading. Curves Indicate Available Elastic Strain Energy to Initiate Fracture.

For the thick specimens, there is almost no strain in the thickness direction as measured by a point micrometer (Figure 23). For these specimens, the plane strain plastic hinge zone is quite narrow and is kept small by the constraint imposed on the zone by the surrounding matrix. Constraint produces a triaxial stress state in the interior of the specimen which can support normal stresses as high as 270 percent of the nominal yield stress (5). In this zone, because of the constraint, the effective stress is too low to allow creation of a large flowed volume. This is due in part to the volume of the sufficiently constrained zone, and also due to the rapid rise in flow stress with strain. Once the crack does start to grow, it is impossible to stop it since a large portion of the total elastic strain energy is available for propagation (Figure 30). Thus, for a plane strain specimen, there should be no chevron arrest. This implies that the number of chevron arrest zones observed on the fracture surface may be a way to define the plane stress-plane strain transition, and therefore a way to determine if a valid plane strain fracture toughness has been calculated. Figures 31 and 32 show the fractography of shear lip and chevron arrest which is ductile.

As seen in Figure 33, the shape, orientation, and size of the chevron arrest zones change with specimen thickness. The changes observed in these zones with an increase in thickness are:

1. The number of arrests decreases exponentially, changing from nine at 0.125 inches to one at 0.477 inches and no arrest for thicker specimens.

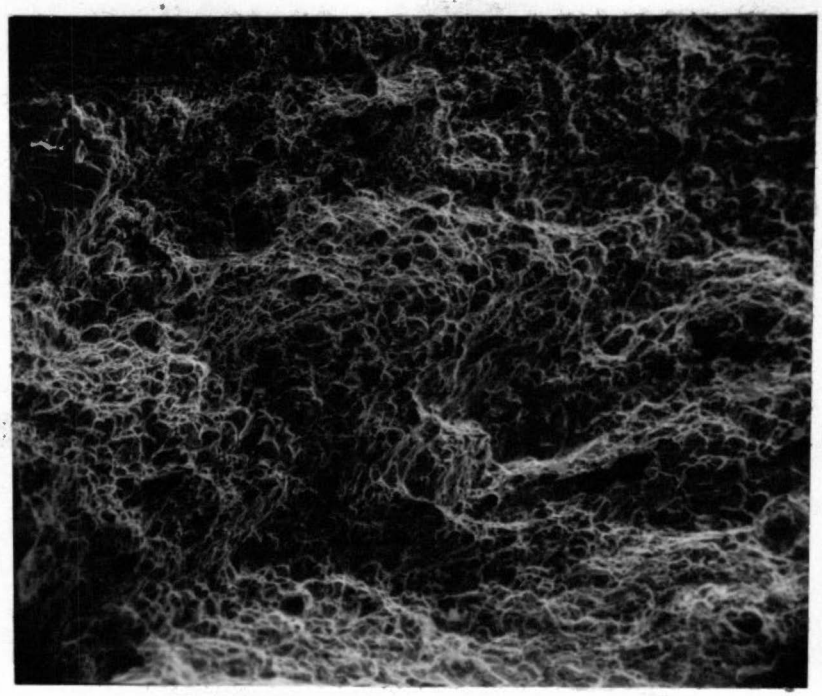

Figure 31. SEM Fractograph of 0.125 Inch Specimen. Area Shows the Shear Lip Which Consists of Ductile Dimpled Fracture. Mag.: 1600X.

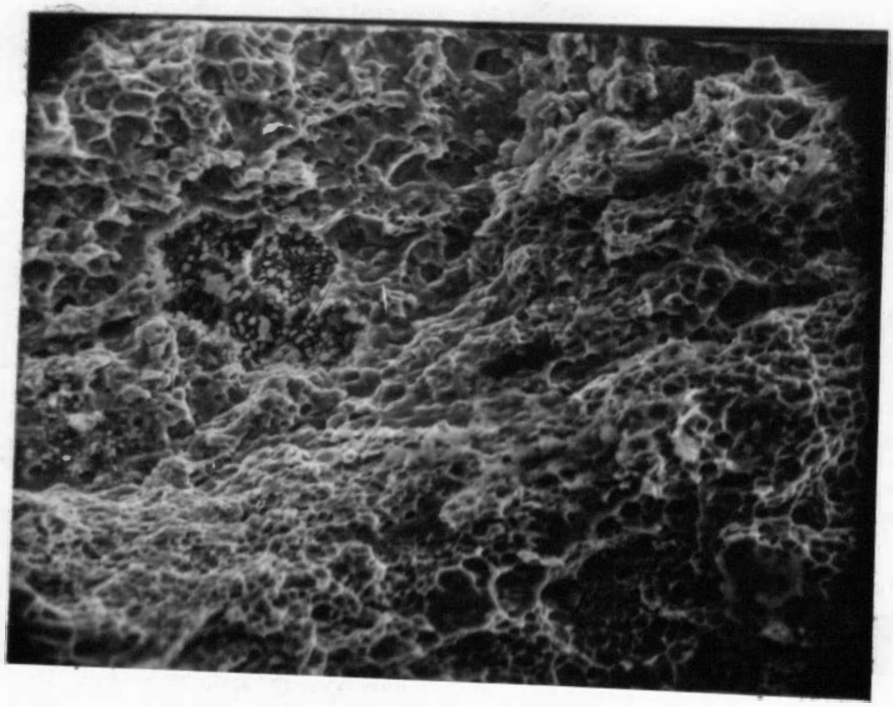

Figure 32. SEM Fractograph of 0.232 Inch Specimen. Area Shows the Chevron Shaped Fracture Arrest Zone Which Consists of Ductile Dimples. Mag.: 1700X.

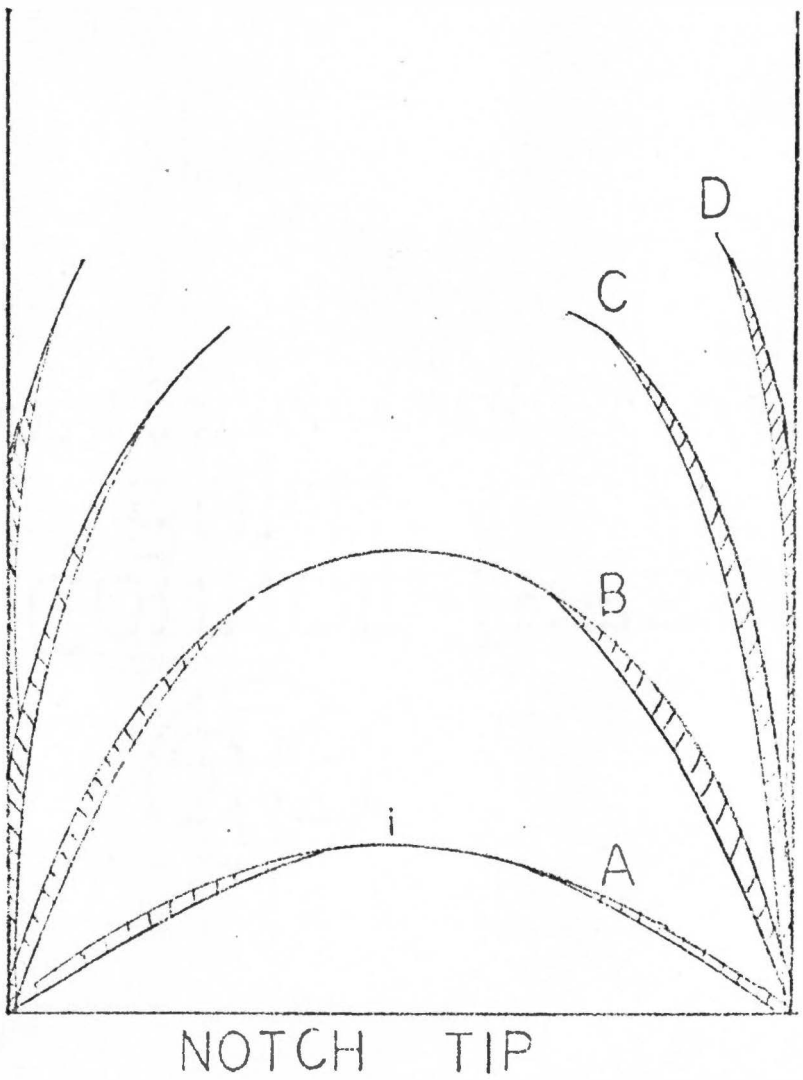

Figure 33. Illustration of Changes in Shape of the Fracture Arrest Zone from Circular to Elliptical to Degenerate as Thickness is Increased. $B_A < B_B < B_C < B_D$

2. The crack length prior to the appearance of the first arrest zone increases.

3. The distance between the n^{th} and $(n + 1)^{th}$ arrest zone decreases as the thickness increases.

As the specimen thickness increases, the constraint at midthickness on the crack plane increases due to the triaxial stress state. Additionally, the amount of constraint at any distance from midthickness on the crack plane also increases as the thickness increases. Therefore, since a critical amount of constraint is required to cause the effective stress to drop below the flow stress and to cause the normal stress to approach the breaking stress, the area on each side of the midthickness unable to flow increases with specimen thickness (Figure 34). In the limiting case, the sufficiently constrained zone becomes equal to the thickness of the specimen. Therefore, the chevron arrest zone visible on the fracture surface--which is the intersection of the plastic hinge and the macroscopic fracture plane--must be absent. Alternatively, for total ductile fracture, the hinge zone in Figure 29 penetrates to midthickness. For intermediate cases, sufficient constraint is present so that the hinge does not penetrate to midthickness. That is, the chevron arrest zone does not penetrate to midthickness on the fracture plane. This causes the arrest zone to change shape from a circular to an elliptical front and finally to degenerate to the shear zone on the side of the specimen. SEM fractography has been used to verify the absence of a hinge zone at midthickness in the

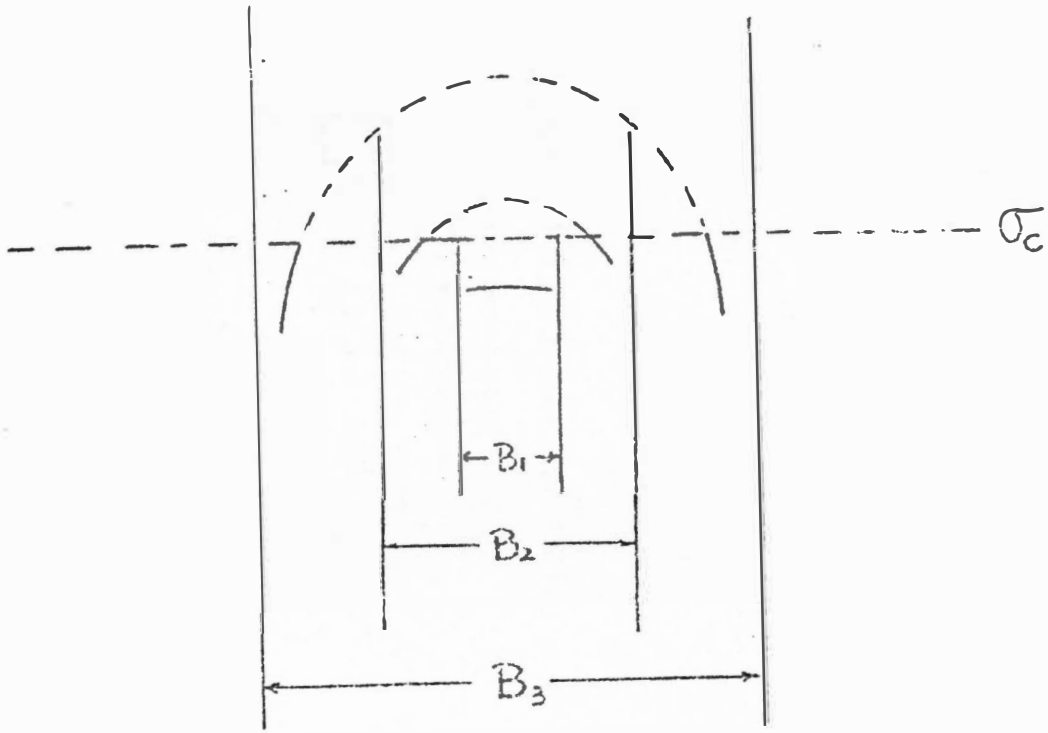

Figure 34. Constrained Stress as a Function of Specimen Thickness Where: $B_1 < B_2 < B_3$ and σ_c = Fracture Stress.

thicker specimens. Figures 35, 36, and 37 show the microscopic fracture surface at midthickness as the thickness increases from 0.125 inches to 1.00 inches. The fracture in this region changes from total ductile fracture to mixed mode to total brittle fracture as the thickness is increased.

Specimens were not sectioned perpendicular to the crack plane to measure the percent slant fracture with thickness, but equivalent results are obtained from macrophotographs of the fracture surface. They show (Figure 38) that the shear lip to total thickness ratio also drops inversely with thickness, decreasing from 20.8 percent at 0.125 inches to 2.5 percent at 0.33 inches to 0.94 percent at 1.00 inches.

Utilizing fractographs obtained by SEM microscopy, it is possible to identify the micromechanisms responsible for fracture. Figure 39 taken on the "flat" portion of the one inch specimen, is typical of brittle fracture and is characterized by cleavage (either steps or river patterns), or by facets. Figure 40 clearly shows the steps, river patterns and microcracks (11). The brittle fracture of the thinner specimens is somewhat different from that observed in the thicker specimens. Figure 41 shows the flat fracture in the 0.232 inch specimen. It is noticed that there are some ductile dimples in addition to the faceting, river patterns, and steps. The dimples are caused by the tearing due to nonuniform strain, and these regions are considered to be the last portion connecting the two fracture surfaces before total fracture. Examination of the

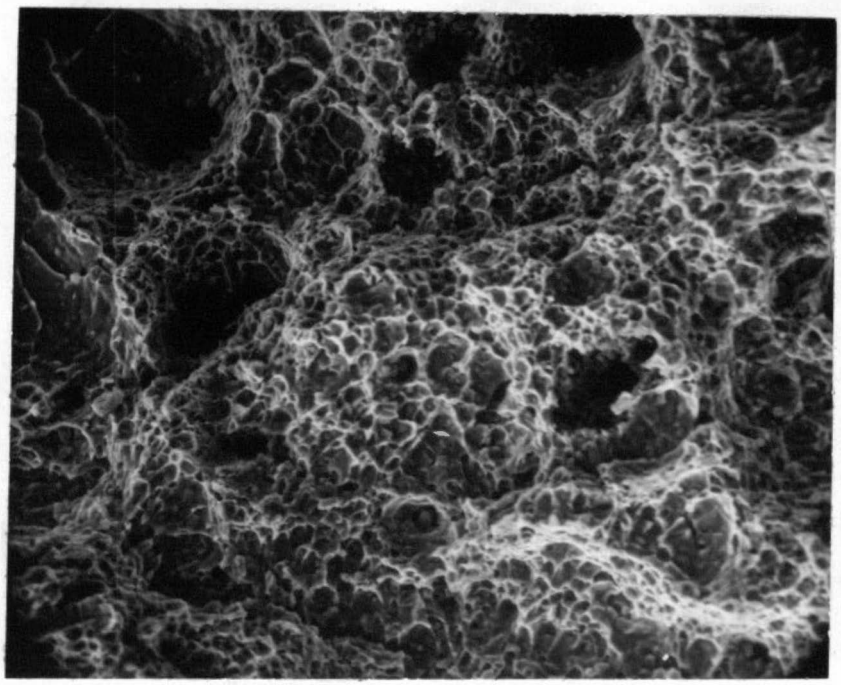

Figure 35. SEM Fractograph of the 0.125 Inch Specimen. Area Photographed Is Region (1) in Figure 33, That Is, at the Juncture of Two Arrest Zones at Midthickness. Mag.: 1000X.

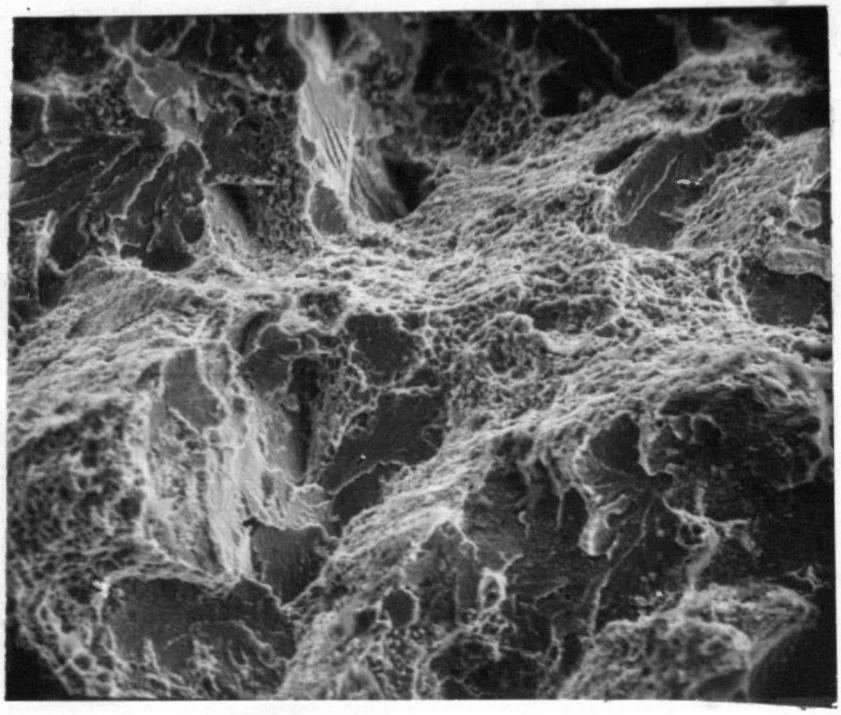

Figure 36. SEM Fractograph of the 0.232 Inch Specimen. Same Area (i) in Figure 35. Mag.: 1600X.

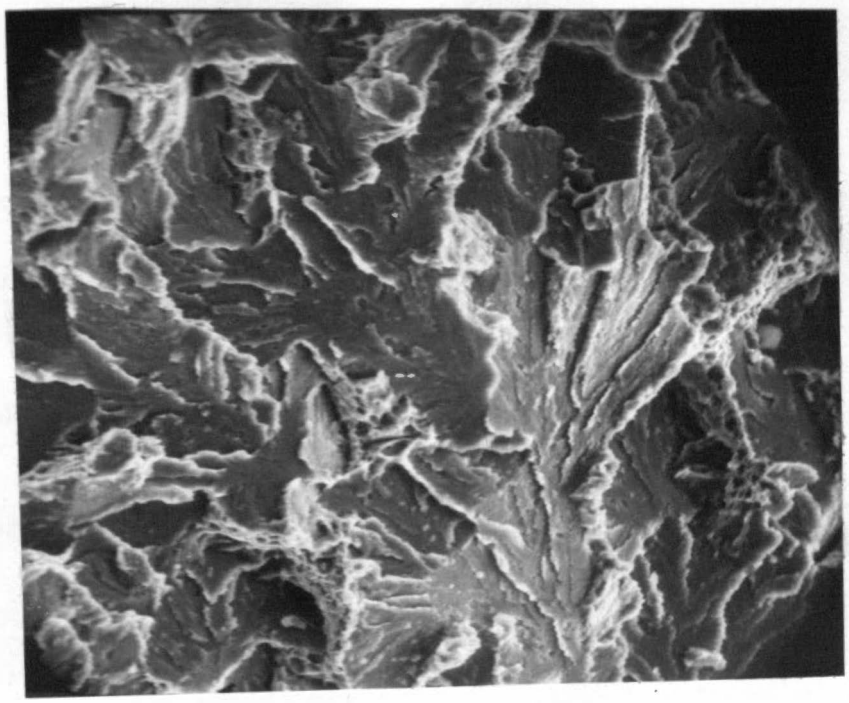

Figure 37. SEM Fractograph of the 1.00 Inch Specimen. Same Area (i) as in Figure 35. Mag.: 1600X.

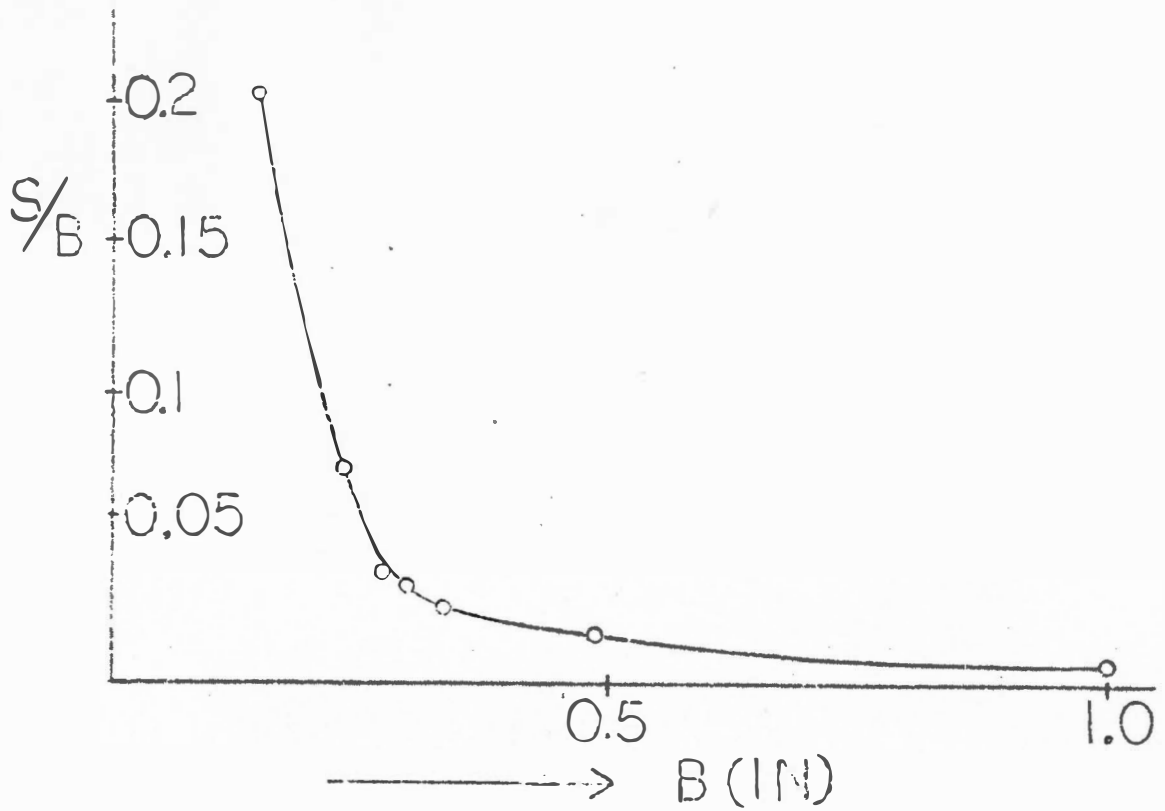

Figure 38. Ratio of Shear Lip Area to Total Thickness (S/B) as a Function of Specimen Thickness. Data Collected from Macrophotographs of the Fracture Surface.

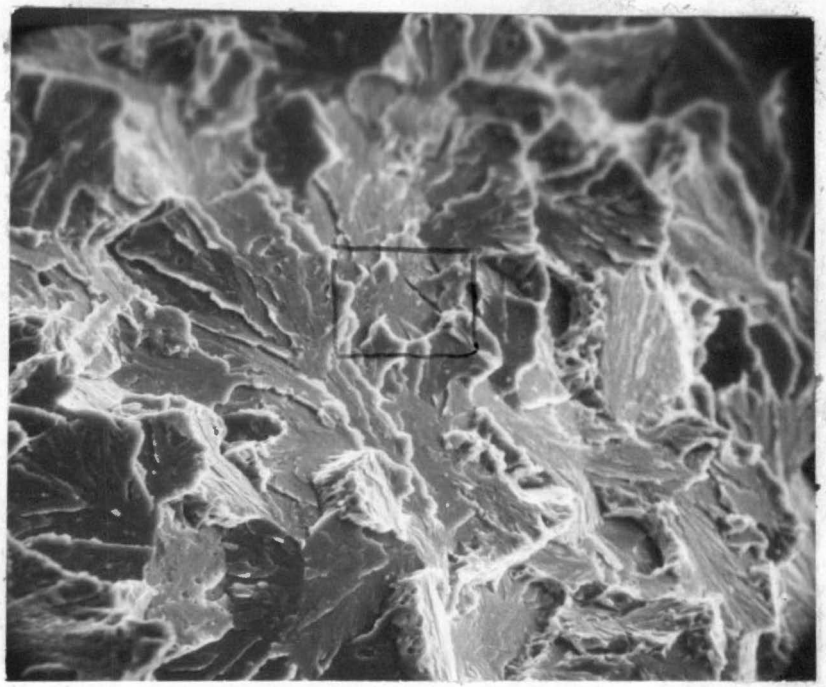

Figure 39. SEM Fractograph of 1.00 in Specimen. Area Shows "Flat" Surface of Brittle Fracture. Mag.: 1600X.

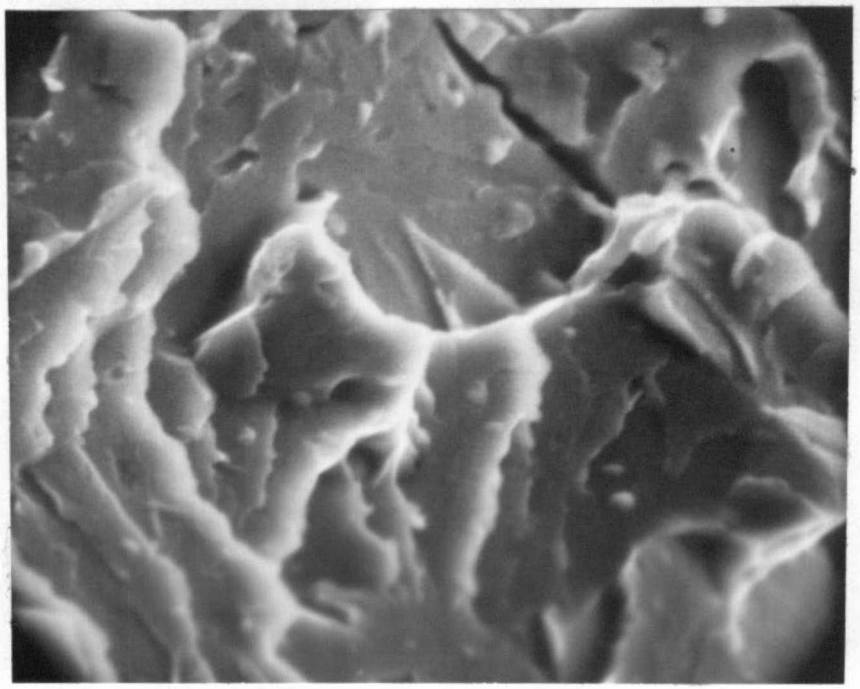

Figure 40. SEM Fractograph of Indicated Region in Figure 39. Area Shows Detail of the Brittle Fracture. Mag.: 8000X.

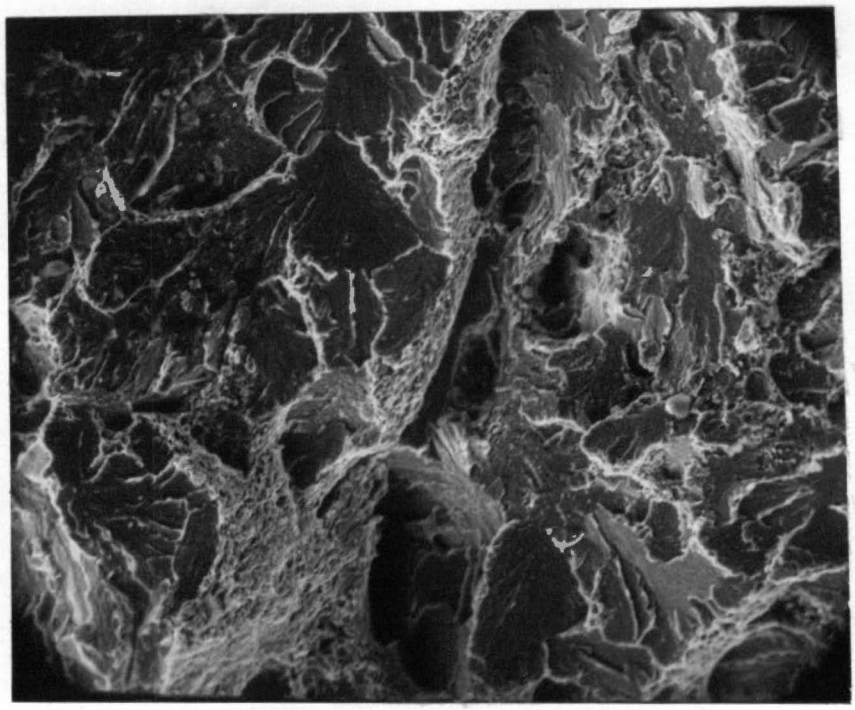

Figure 41. SEM Fractograph of the 0.232 Inch Specimen. Area Shows a Macroscopically Flat Fracture Surface Which Contains Dimples.

thinner specimens (e.g., at 0.125 inches in Figure 42) reveals that the fraction of dimples in the thinner specimens is higher than is indicated by the macrophotograph of the fracture surface in Figure 20. That is, data from Figure 20 was obtained by cutting and weighing portions of the macrophotographs corresponding to the macroscopic ductile and brittle regions. However, SEM data indicate some dimples with the brittle area which cannot be resolved in the macrophotographs.

Figures 43, 44, and 45 show the PIZ hinge zone of different magnifications at 0.477 inch specimen. The two photographs at lower magnification show a well defined transition from ductile to brittle fracture, and the highest magnification shows the detail of the ductile dimple fracture. Figure 46 shows the intersection of shear lip and chevron arrest at low magnification. Figure 47 shows the plan view surface in the vicinity of shear lip and indicates that the void-like holes were formed as the stress increased, and then connected to each other by breaking through the plan view surface. Figure 48 shows another mixed mode fracture for the 0.232 inch specimen. Figure 49 is at a higher magnification and shows a mixture of voids formation and cleavage. Figure 50 shows a tearing ridge from the 0.477 inch specimen, and which shows the brittle fracture in the background. Figure 51 shows the tear ridge itself is one of ductile dimples.

Based on shear lip data, the mixed mode to brittle transition essentially occurs in the 0.330 inch specimen. SEM data indicate,

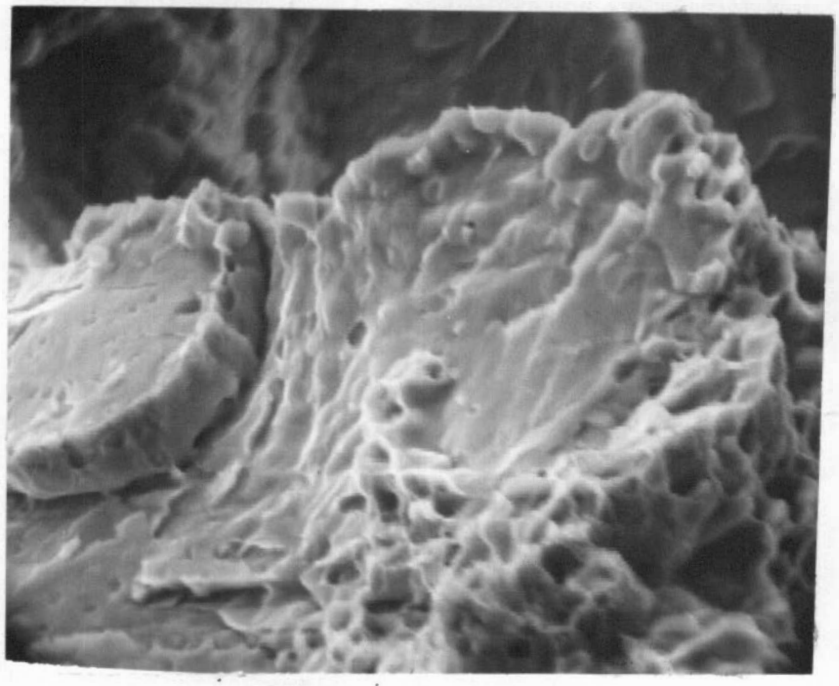

Figure 42. SEM Fratograph of the 0.125 Inch Specimen, Area in Flat Region, but Again Shows Dimples.

Figure 43. SEM Fractograph of the 0.477 Inch Specimen. Photograph Shows the Plastic Initiation Zone Adjacent to the Crack Starter Notch.

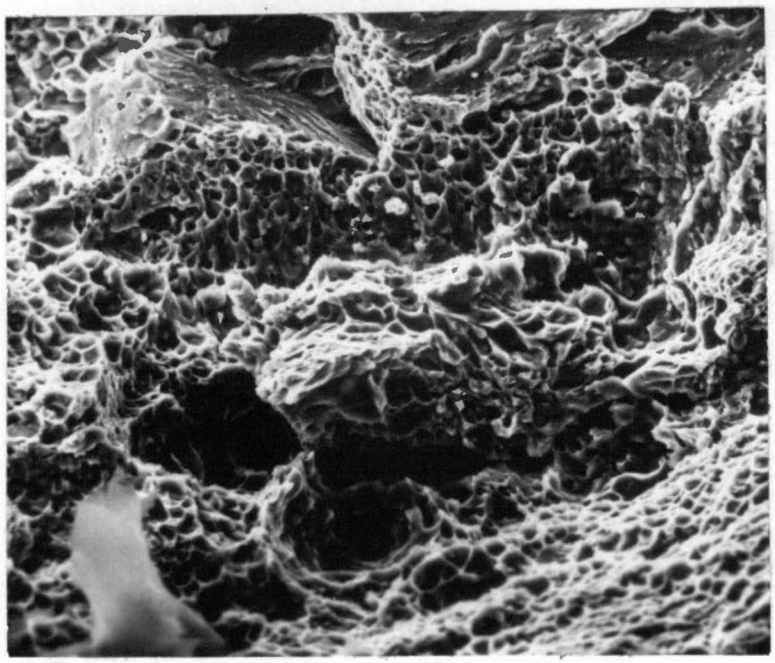

Figure 44. SEM Fractograph at the Center of Figure 43 Showing the Transition from Ductile to Brittle Fracture. The Region Indicated Is an Artifact.

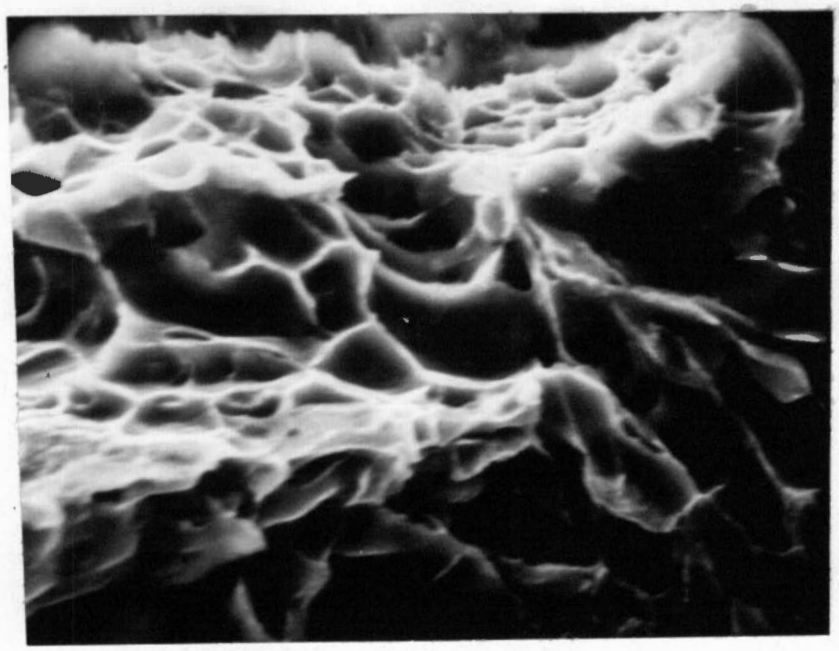

Figure 45. SEM Fractograph at the Center of Figure 44 Showing Details of the Observed Ductile Fracture.

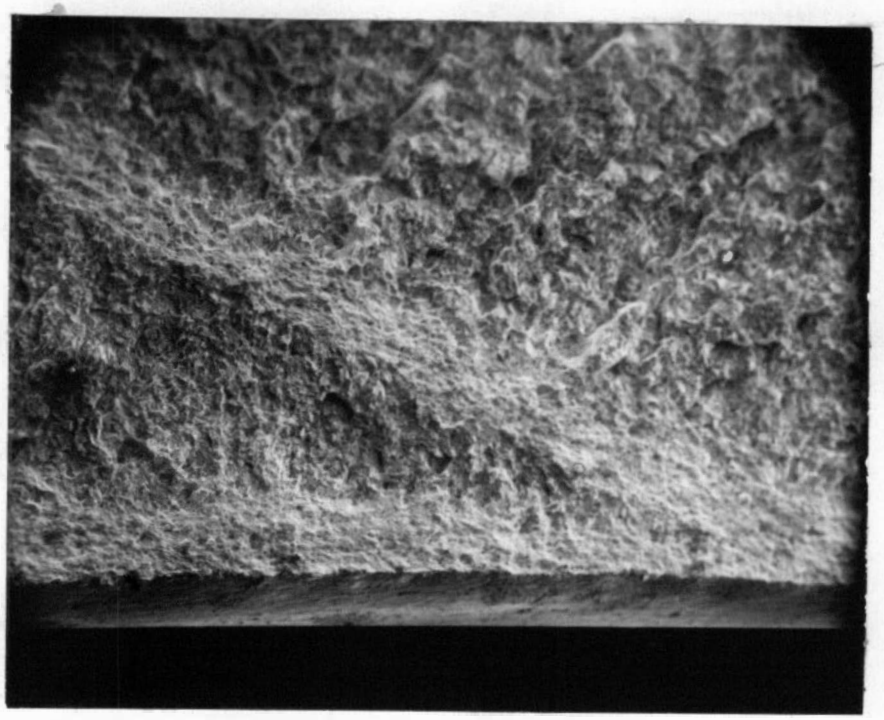

Figure 46. SEM Fractograph of the 0.125 Inch Specimen. Photograph Taken at the Intersection of the Shear Lip and an Arrest Zone. Mag.: 45X.

Figure 47. SEM Fractograph of the 0.125 Inch Specimen. Photograph Taken at the Plan View Surface in the Vicinity of the Shear Lip. Mag.: 2000X.

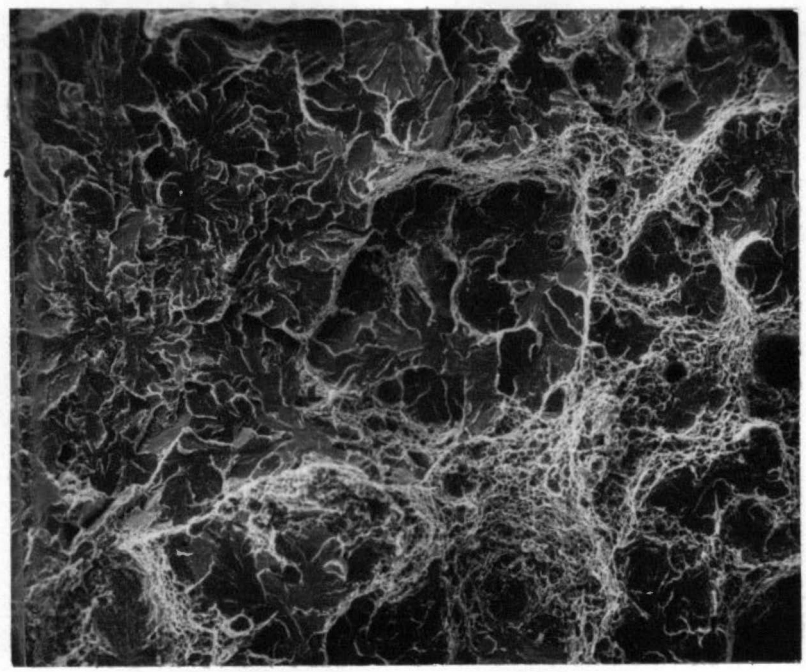

Figure 48. SEM Fractograph of the 0.232 Inch Specimen. Area Photographed Near the Intersection of Two Arrest Zones at Specimen Midthickness. Mag.: 450X.

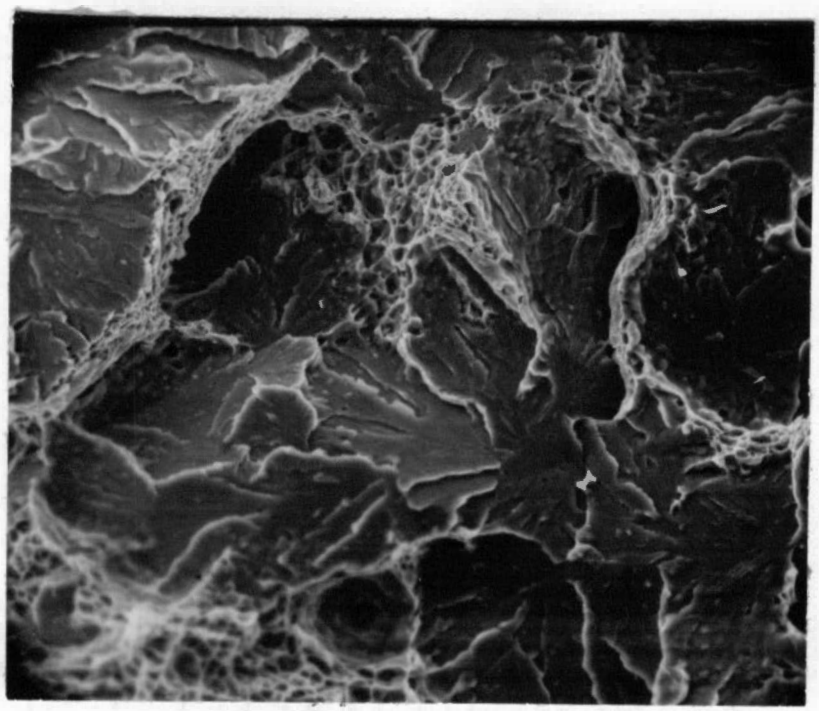

Figure 49. SEM Fractograph of the Center Region in Figure 48, Showing Mixed Mode Fracture.

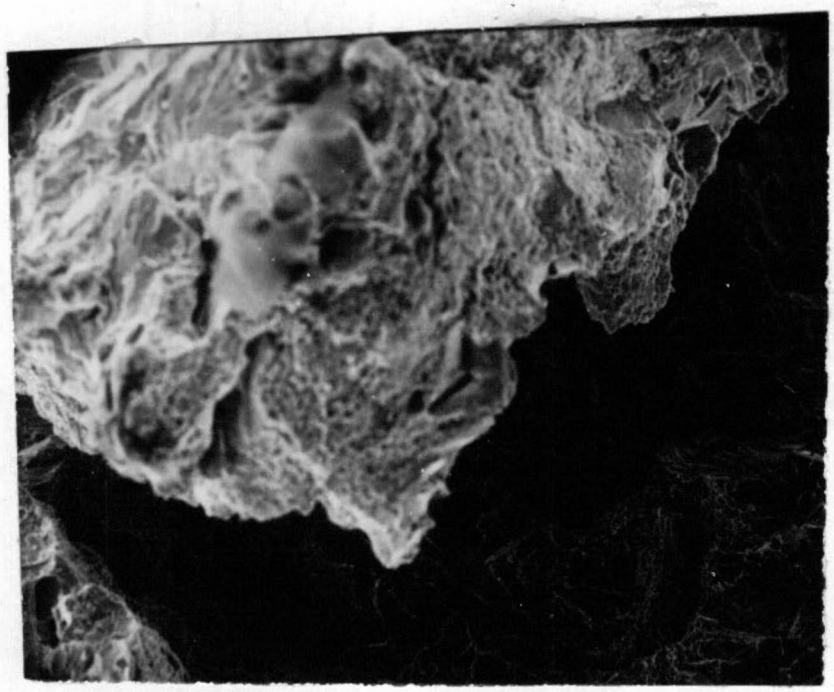

Figure 50. SEM Fractograph of the 0.477 Inch Specimen. Photograph Taken in the Flat Fracture Region Away from Shear Lip Zone, Plastic Initiation Zone, and Arrest Zone. Mag.: 450X.

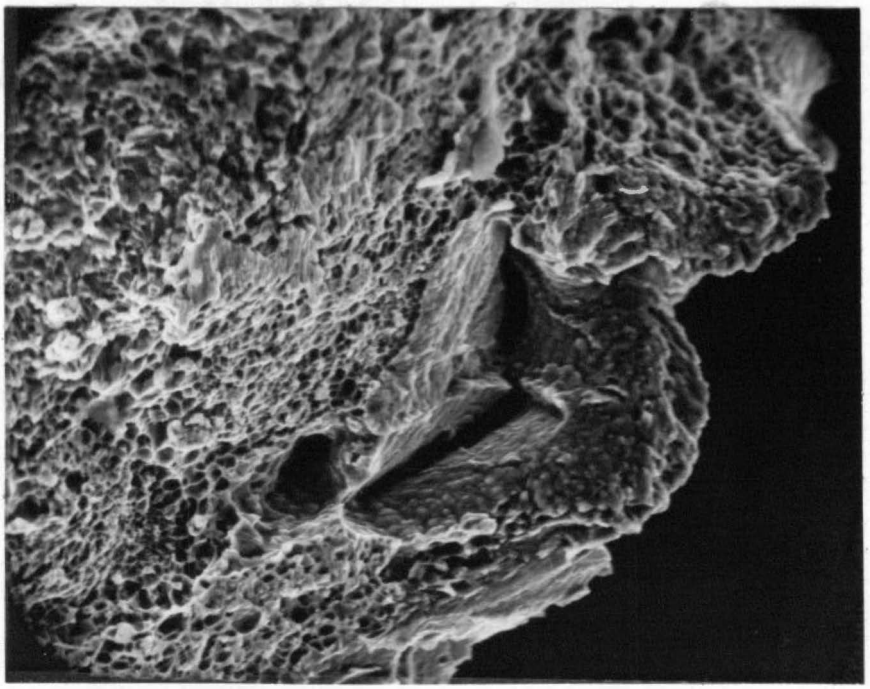

Figure 51. SEM Fractograph at the Center of Figure 50 Showing a Tear Ridge Structure. Mag.: 1800X.

however, that even though the fracture surface is flat at 0.477 inches, crack propagation was partially ductile. This may not be inconsistent since Figure 38 does indicate about one percent shear for the 0.323 and 0.477 specimens.

Comparison of Fracture Transitions Based on P-COD Data and Strain Measurements

All strain measurements recorded and discussed in the previous section, as well as SEM data, indicate that a fracture transition from mixed mode to brittle mode occurs within the specimen thickness range used in this work. Yet, load-COD data do not indicate pop-in for these specimens, and in fact, well defined pop-in did not occur in the 1.00 inch thick specimen. Of the four one inch specimens tested, two specimens gave an indication of pop-in.

These are observed in spite of the linearly increasing values of P_p and P_m fracture mode transitions from the thinnest to thickest specimens. These observations are not in agreement with the general observation that ductile fracture absorbs more energy than brittle fracture (i.e., large loads are required for ductile fracture) such as shown in Figure 17. Furthermore, these results imply that total brittle fracture on a microscopic scale (as revealed by SEM) may not correspond to macroscopic definitions of plane strain loading for a material that shows a 25 percent elongation and 50 percent reduction in area (i.e., not an inherently brittle material).

Fracture Toughness Data and ASTM E-399 Test Requirements

Based on the load-COD data, the equation used to calculate

fracture toughness is given as (9):

$$K_Q = P_Q[f(a/w)] \; / \; B(w)^{1/2} \qquad (7)$$

where:

$$f(a/w) = 29.6\,(a/w)^{1/2} - 185.5\,(a/w)^{3/2} + 655.7\,(a/w)^{5/2}$$
$$- 1017.0\,(a/w)^{7/2} + 638.9\,(a/w)^{9/2}$$

As mentioned before, P_Q is the secant modulus intercept load. The variation of K_Q with thickness is shown in Figure 52. The apparent fracture toughness based on maximum load (K_m) and proportional load (K_p) are also shown in Figure 52. All data indicate that the apparent fracture toughness is constant if pop-in did not occur, and is increased with thickness if pop-in occurred. This result is quite surprising since it argues that the minimum energy for crack initiation increases as the fracture mode changes from mixed to 98 percent brittle fracture (as indicated by SEM), and brittle fracture presumably absorbs less energy than ductile fracture.

Several authors have reported increasing fracture toughness values with an increase in plate thickness (6, 7, for example). However, these results are identified as ductile mode, and occur for thicknesses less than that specified by ASTM E-399 (i.e., B, a $\leq 2.5 \left(\frac{K_{Ic}}{\sigma_{ys}}\right)^2$).

May (12) has reported, however, an increase in K_Q with thickness for Hylite 50 (a titanium alloy) for thicknesses and starter

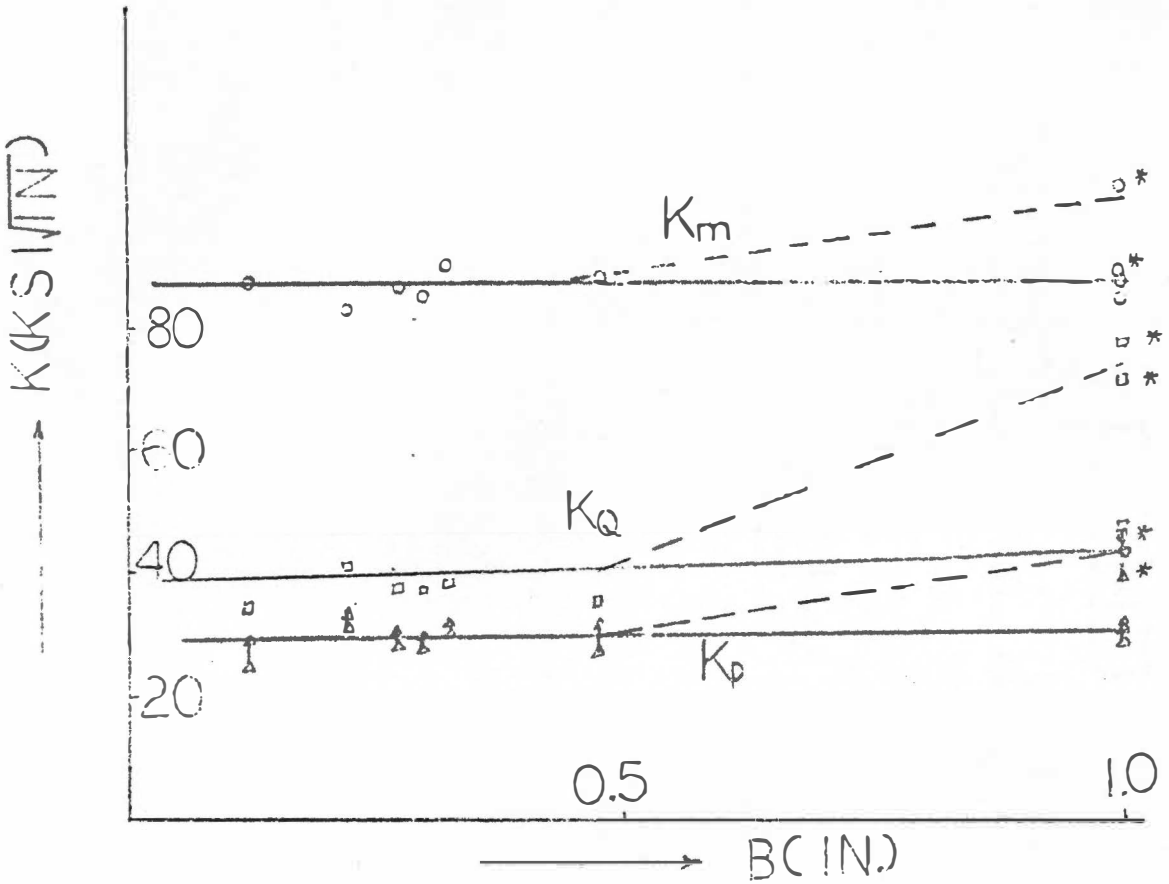

Figure 52. Values of Fracture Toughness as a Function of Thickness Based on Maximum Load (Km), Secant Intercept Load (K_Q) and Proportional Load (K_p), where * Indicates Pop-In.

crack lengths meeting ASTM thickness and crack length criteria. Unfortunately May does not report macro or microscopic evidence of crack growth mode. Kaufman (13) has reported similar results for a hardening aluminum alloy (7075-T7351), but again the fracture mode is not reported. Consequently results of this work (and possibly those of May and Kaufman) imply that the generally accepted criterion that the crack length and plate thickness be greater than 2.5 $(K_{Ic}/\sigma_{ys})^2$ may be invalid, even for materials that show unnotched tensile ductility.

A plausible explanation for results of the present work does exist. Since specimens were produced such that all dimensions were the same except thickness, and only the one inch specimen met ASTM standards, then only data obtained from the one inch specimen can legitimately be utilized in Equation (7) to calculate K_Q. This equation should not apply directly to thinner specimens unless a correction factor is added to obtain the appropriate value of K_Q.

In order to obtain this correction factor, the crack length of those thinner specimens should be comparable to the thickness-B, or $a \tilde{=} B$. This is equivalent to moving the loading pin position (d) to (f) (Figure 53).

If we assume the moment from the pin hole to the crack tip is constant, M, then:

$$P_1 \cdot a_1 = M = P_2 \cdot a_2$$

$$\text{since } a_1 = 1", \quad a_2 = B \tag{8}$$

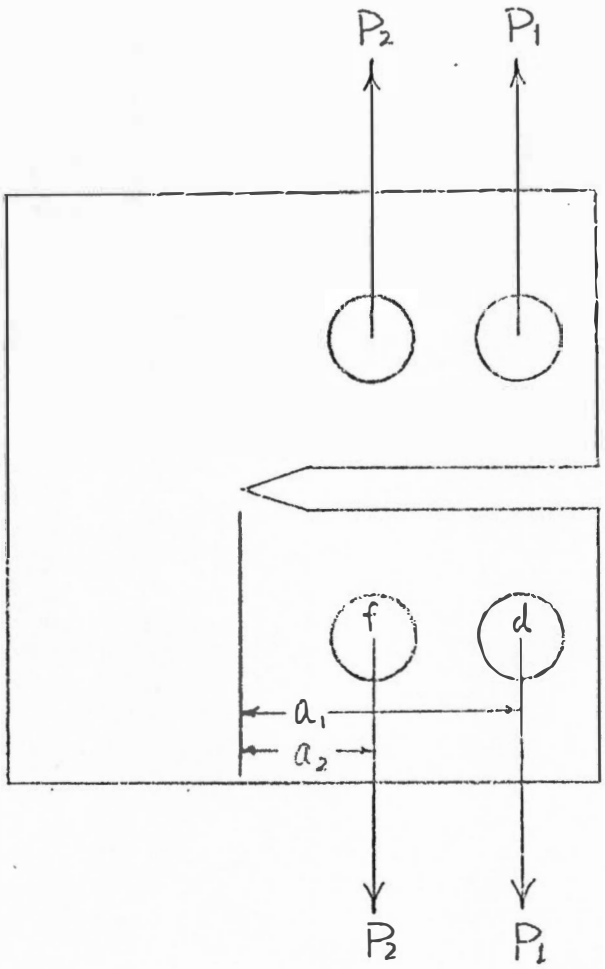

Figure 53. Movement of the Loading Pin Position from (d) to (f) Based on Equal Moment at the Crack Tip.

and $P_2 = P_1/B$ (9)

Then substituting Equation (8) and Equation (9) into Equation (7), we obtain

$$K_Q = P_Q \cdot [f(a/w)] / B^2 \cdot (W)^{1/2} \quad (10)$$

If Equation (10) is then applied to calculate the K_Q value for those thinner specimens, we obtain the result shown in Figure 54. This corrected plot of K_Q is then in agreement with SEM data as well as all strain indications of the fracture transition. However, it should be noted that the width of the thinner specimens is still too large for the thickness. This is expected to have an effect on fracture mode, only if the width is insufficient to hold the plastic zone size to less than the width of the specimen. For specimens used in this study, the width of the thinner specimens was greater than the required ratio of $2a \leq w$. Therefore, this parameter is not expected to affect calculated results based on equivalent moment arms.

With the large amount of interest in the past few years in measuring fracture toughness, ASTM specifications for standardized evaluation procedures have seen almost yearly changes. Several criteria have been proposed to decide whether a valid plane strain experiment has been performed:

1. $a \geq 2.5 \, (K_{Ic}/\sigma_{ys})^2$ (9)

2. $B \geq 2.5 \, (K_{Ic}/\sigma_{ys})^2$ (9)

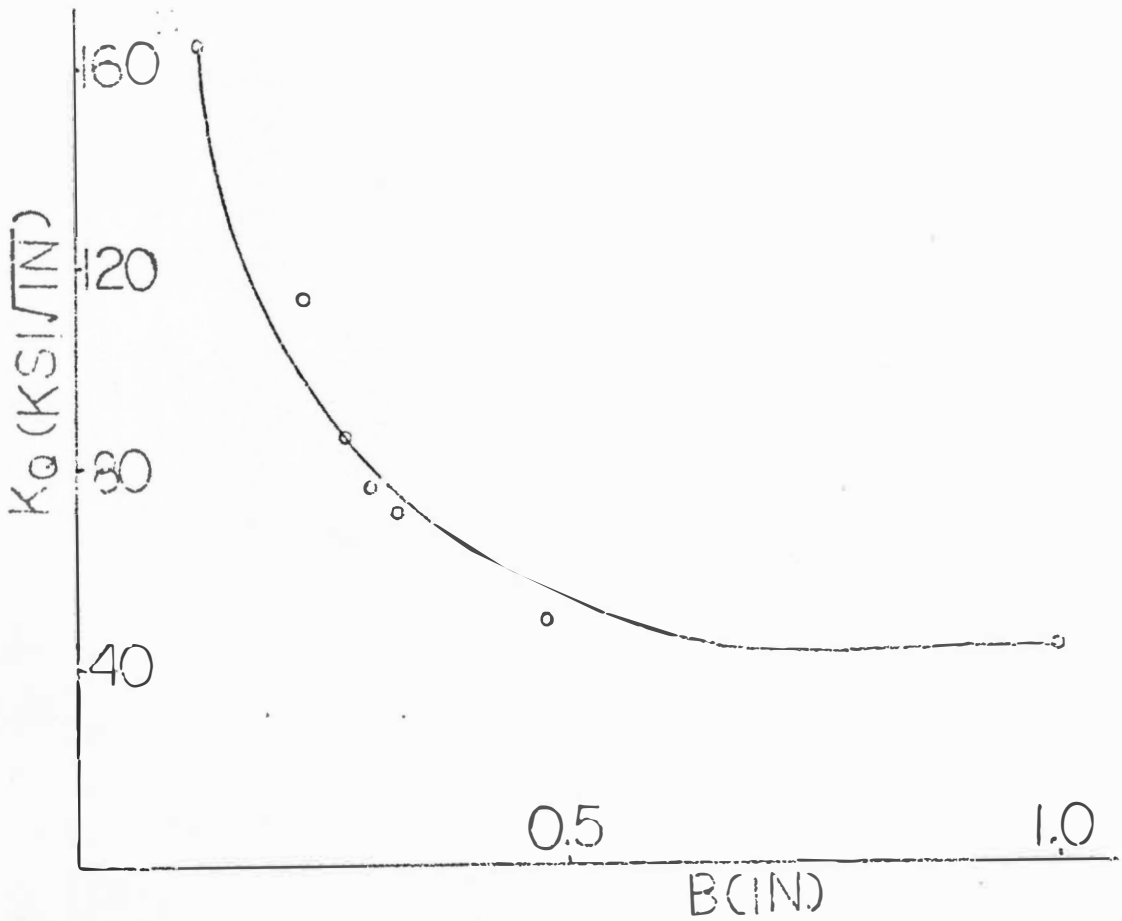

Figure 54. Corrected Fracture Toughness as a Function of Thickness Based on Correction Factor Method.

3. The occurrence of "pop-in" in the course of the test (9)

4. $P_m/P_Q < 1.1$ (9)

5. The absence of shear lip formation and a crack plane normal to the applied load. (1)

These five criteria are all attempts to insure that the state of stress created by geometrical constraint is adequate to make a potentially ductile material fail in a brittle manner. Implied, but not stated directly is that the fracture mechanism be brittle. It is also inherently assumed that a brittle mechanism of crack propagation requires less energy than a ductile mechanism. Stated differently, criteria for a valid plane strain test are based on macroscopic observations that are supposed to guarantee a microscopic mode of crack growth. For example, criterion (5) inherently assumes that the presence of lips on the side of the fracture surface are evidence of ductile flow--the origin of the term "shear lips;" so that it is impossible for brittle fracture to occur on any plane other than that one which is normal to the load. This brings to mind inherent difficulties in describing fatigue fracture. From a macroscopic viewpoint, little or no gross plastic strain is associated with the failure, so that the fracture might be described as brittle. Yet on a microscopic scale, there is ample evidence of intense localized plastic deformation, so that the failure is at least accompanied by, or initiated due to, ductile mechanisms.

Some materials are incapable of ductile fracture whether

geometric constraint is imposed or not, and for these materials, the lower bound crack propagation energy is measured whether or not the above criteria are met. However, for all other classes of materials, it is important to guarantee that the minimum energy for crack propagation is measured, and that the criterion for this decision is valid. Again, with reference to criterion (5), it must be known whether the appearance of a macroscopic fracture plane inclined to the load axis implies a ductile mode of crack propagation, or that a flat plane guarantees brittle mode.

Items (1) and (2) are based on experimental results which have indicated that if crack length and thickness were approximately 50 times the radius of the theoretical plastic zone, relatively high assurance existed that plane strain I.e., "brittle") conditions had been achieved. This imposes a severe experimental limitation since it requires very thick specimens to measure K_{Ic} in inherently tough materials. From our data, if we assume that the correction factor obtained from an adjusted moment arm method is correct, then 2.5 $(K_{Ic}/\sigma_{ys})^2$ = 1.6 inches which is larger than the K_{Ic} thickness of present work (less than on inch). Other references (5, 13, for example) also support the opinion that criteria (1) and (2) are too severe. It is now accepted that this criterion is conservative and attention has been focused on procedures that might allow the testing of thinner specimens. If temporary load instability occurs during loading so that the crack propagates instantaneously for some distance (i.e., "pop-in," see Figure 1, page 6), it is accepted

that data for the test is valid to calculate K_{Ic}. However, it is also possible to measure K_{Ic} without pop-in based on empirical and experimental observations (Figure 2, page 8). The implication is that pop-in would occur in a thicker specimen. From the present results obtained in this work, the occurrence of pop-in only increases the apparent fracture toughness!

Macroscopic toughness calculations based on ASTM E-399 predict an apparent fracture toughness dependance on crack length and specimen thickness as shown in Figure 6. The minimum value at $B > B_c$ or $a > a_c$ is taken to be the plane strain (brittle) value, while the maximum apparent value is taken to be the plane stress (ductile) value. Considerable data exist to argue that the plane stress value is accompanied by 100 percent oblique fracture, that the K_{Ic} value is accompanied by no oblique fracture, that the fracture appearance varies continuously between K_C and K_{Ic} (mixed-mode) and that fracture for $B < B_c$ or $a < a_c$ is 100 percent oblique. As previously mentioned, these macroscopic observations assume microscopic modes of crack propagation. Flat fracture occurs only by a brittle mechanism and slant (oblique) fracture occurs only by a ductile mechanism.

There are in fact two microscopic modes of crack propagation which could result in an apparent macroscopic brittle fracture--general cleavage and void coalescence and/or microcrack formation on the crack plane in advance of the main crack front. That is, fracture could occur by advance of the crack front from the starter notch, or by the primary crack jumping across non-failed areas

connecting microcracks or voids in front of the primary crack tip.

SEM data in this work does show that it is possible for ductile mechanisms to operate on a macroscopically flat fracture plane.

It was observed that this flat fracture plane was always normal to the applied load. Fracture that occurred on macroscopic oblique planes was observed to occur only by a ductile mechanism. That is, macroscopic oblique fracture occurred only by ductile mechanisms but fracture on the macroscopic plane normal to the load occurred by both ductile and brittle mechanisms. Fracture arrest on the flat plane occurs by a ductile mechanism, but this is visible to the naked eye on the macroscopic plane normal to the load. The point is that, even in the absence of visible arrest on this plane, fracture may partially occur by ductile mechanism. The relative amount of ductile fracture on the normal plane does decrease as the thickness is increased. This implies that minimum thicknesses required to produce "flat" fracture are not sufficient to guarantee totally brittle fracture on a microscopic scale. This in turn implies that minimum thicknesses to obtain a valid K_{Ic} fracture toughness are larger than that predicted by plots of percent flat fracture versus thickness.

Pellini (14) suggests that void coalescence to form microcracks in front of the main crack tip is more likely as opposed to general cleavage for low ratios of K_{Ic}/σ_{ys}, but gives no numerical values of this ratio. SEM data in this work substantiate Pellini's

argument and indicate void nucleation on the crack plane adjacent to carbide particles. K_{Ic}/σ_{ys} for this work is 0.8 for moment arm corrected data, or between about 0.55 and 1.3 for the uncorrected data.

As Pellini clearly points out, crack initiation should be considered a strain limiting rather than stress limiting criterion, and that K_{Ic} is an attempt to describe the initiation of a crack in a constrained volume. If crack initiation does not result in propagation across the total cross section, the strain energy release rate (G_c) is better able to describe crack propagation.

The use of K_{Ic} to describe fracture resistance is popular since it predicts toughness in terms of a stress parameter which can be treated analytically. Analytical mechanics is presently unable to treat a strain criterion for fracture in a material which shows elasto-plastic behavior.

In practice, measurement of K_{Ic} requires a series of specimens of varying thickness, the maximum thickness being limited by the machine load capacity, the difficulties inherent in handling thick sections, and the difficulty in obtaining a constant microstructure with section thickness (which may approach six inches, eight inches, or even greater).

Present data indicate that the K_{Ic} value is not necessarily accompanied by zero percent oblique (ductile) fracture (although it is less than one percent) if the assumed correction factor method is right.

With respect to criterion (4), the ratio of P_m/P_Q in this work is close to 1.5 instead of 1.1.

CHAPTER V

CONCLUSIONS AND RECOMMENDATIONS

Conclusions

The following conclusions can be drawn from the present work:

1. The transition from ductile to brittle behavior on the microscopic scale of the material is equivalent to the transition from plane stress to plane strain behavior on the macroscopic scale for all criterion except the criterion that the PZS on the plan view be two percent of the thickness. A correction factor has been applied to the data from this work, based on proportional moment arms, in order to force K_{Ic} to decrease with thickness, rather than to increase. Additional substantiation of this behavior should be obtained. However, these transitions occur for thicknesses considerably less than that required by ASTM E-399 criterion.

2. The changes of the number of the chevron arrests, the plastic zone sizes, shear lips area, ductile fraction of fracture surface with changing specimen thickness are good indications of the microscopic ductile-brittle transition.

3. The apparent fracture toughness increases or remains constant as the thickness is increased if calculated by Equation (7) but it decreases as the thickness is increased if a correction factor is applied by using Equation (10).

4. The existing criteria for a valid K_{Ic} test have been shown

to be overly conservative, except those criteria utilizing the PZS on the plan view and the percent flat fracture versus thickness. The latter two criteria have been shown to be inadequate. The PZS criterion need not be met to produce total brittle fracture on a microscopic scale. SEM data indicate that the minimum thickness to give 100 percent "flat" fracture is less than the minimum thickness required to give 100 percent brittle fracture on a microscopic scale.

Recommendations

A number of recommendations can be made at this time for the understanding of fracture behavior and through which more refined criteria for valid K_{Ic} testing may be developed.

1. Since the fracture testing is notch sensitive, the three mil notch radius is sufficiently large that it may require more energy to initiate cracks than a smaller notch radius. Therefore, it is recommended that specimens be pre-fatigue cracked to minimize the notch effect. K_{Ic} is in reality a measure of the requirements of minimum energy for crack initiation followed by propagation. Therefore, it is necessary to obtain a minimum notch radius, which must be standardized, if the apparent stress intensity required to obtain a fracture surface (i.e., after propagation and which is microscopically brittle) is to be a true material constant. Current minimum (and standardized) notch radii are prepared by fatigue loading.

2. SEM microscopy must be applied more intensively by

workers to justify microscopic mechanisms with observed macroscopic behavior to assure that a ductile mode of propagation does not occur on the macroscopic crack plane normal to the load. This implies, again, the importance of a strain criterion for fracture.

3. An evaluation program using materials of constant K_{Ic} but different strain hardening coefficients would clarify the importance of strain on the fracture plane in controlling the mode of propagation. This is of critical importance since macroscopic appearance of the fracture plane is used to decide the validity of an initiation event.

REFERENCES

REFERENCES

1. Srawley, J. E. and W. F. Brown, "Fracture Toughness Testing," ASTM STP-381, 1965.

2. Griffith, A. A., "The Phenomena of Rupture and Flow in Solids," Philosophical Transactions Royal Soc., Series A., Vol. 221, 1920.

3. Irwin, G. R., "Onset of Fast Crack Propagation in High Strength Steels and Aluminum Alloys," NRL-Report-4763, 1955.

4. McClintock, F. A. and G. R. Irwin, "Plasticity Aspects of Fracture Mechanics," ASTM STP-381, 1965.

5. Hahn, G. T. and A. R. Rosenfield, "Source of Fracture Toughness: The Relation Between K_{IC} and the Ordinary Tensile Properties of Metals," ASTM STP-432, 1968.

6. Brothers, A. J. and S. Yukawa, "Fracture Test Methods and Their Application," AIME Symposium, Vol. 31, 1966.

7. Sullivan, A. M. and J. Stoop, "Effect of Sheet Thickness on the Fracture Resistance Parameter K_c for Steels," NRL Report 7601, 1973.

8. Becker, W. T., Supplementary Notes on Fracture, Chem. and Met. Engr. Dept, Univ. of Tennessee.

9. ASTM Committee E-74, E-399, Part 31, ASTM Standard, 1972.

10. Taggart, R., D. H. Polonis and L. A. James, "Plastic-Strain Distribution at the Root of a Sharp Notch," Exp. Mech., 7(9), September 1967.

11. Beachem, C. D. and R. M. N. Pelloux, "Electron Fractography--A Tool for the Study of Micromechamisms of Fracturing Processes," ASTM STP-381, 1965.

12. May, M. J., "British Experience with Plane Strain Fracture Toughness Testing," ASTM STP-463, 1970.

13. Kaufman, J. G., "Fracture Toughness Testing," ASTM STP-476, 1970.

14. Pellini, W. S., "Evaluation of Engineering Principles for Fracture-Safe Design of Steels Structures," NRL Report-6957, September 1969.

VITA

The author, Wun-Sen Lin, was born in Taichung, Taiwan, on January 10, 1947, the second son of Mr. and Mrs. Wei-Song Lin.

The author attended Taichung First High School where he graduated in 1965. He then entered National Cheng Kung University, where he received a B.S. degree in Engineering Science in 1969. As an undergraduate, the author received a scholarship sponsored by the Chinese Technical Service. He worked for Metal Research Industries Institute, Taiwan, from July 1970 to August 1971. He then came to the United States, and after studying at the Georgia Institute of Technology for one semester, transferred to the University of Tennessee in March 1972.